Am J Physiol Cell Physiol 329: C1792–C1809, 2025.
First published October 21, 2025; doi:10.1152/ajpcell.00254.2025

american physiological society

AMERICAN JOURNAL OF PHYSIOLOGY
CELL PHYSIOLOGY

RESEARCH ARTICLE

Dynamic time course of muscle proteome adaptation to programmed resistance training in rats

Connor A. Stead,[1] Stuart J. Hesketh,[1] Aaron C. Q. Thomas,[1,2] Mark R. Viggars,[1] Hazel Sutherland,[1] Jonathan C. Jarvis,[1] and Jatin G. Burniston[1]

[1]*Research Institute for Sport & Exercise Sciences, Liverpool John Moores University, Liverpool, United Kingdom and*
[2]*McMaster University, Hamilton, Ontario, Canada*

Abstract

Resistance training promotes muscle protein accretion and myofiber hypertrophy, driven by dynamic processes of protein synthesis and degradation. Muscle adaptations to ongoing resistance training occur over weeks, but most molecular knowledge on the process of adaptation is derived from static measurements at specific time points, which do not capture the dynamics of the adaptation process. To address this, we utilized deuterium oxide labeling and peptide mass spectrometry to quantify absolute protein content (grams) and synthesis rates (grams/day) in skeletal muscle during a time series experimental design. A daily programmed resistance training regimen was applied to male rat tibialis anterior via electrical stimulation of the left hindlimb for 10, 20, and 30 days (5 sets of 10 repetitions daily). Muscle samples from stimulated and contralateral control limbs were analyzed, quantifying 658 protein abundances and 215 protein synthesis rates. Unsupervised temporal clustering of protein responses revealed distinct phases of muscle adaptation. The early (0–10 days) response was driven by greater rates of ribosomal protein accretion and the mid (10–20 days) response by expansion of mitochondrial networks. These findings highlight that subsets of proteins exhibit distinct adaptation timelines due to variations in translation and/or degradation rates. The new understanding of temporal patterns highlighted by our dynamic proteomic data helps interpret static data from studies at isolated time points and could improve the development of strategies for optimizing muscle growth and functional adaptation to resistance training.

NEW & NOTEWORTHY We used stable isotope labeling and proteomic analyses to quantify absolute changes in the synthesis and abundance of muscle proteins during programmed resistance training in rat in vivo. This novel time-resolved approach revealed distinct phases of adaptation, characterized by early ribosomal and later mitochondrial protein accretion. Strikingly, we observed substantial "oversynthesis" of muscle proteins; that is, the net gain in muscle protein content was much less than the amount of newly synthesized protein.

deuterium oxide; exercise; muscle; protein synthesis; proteomics

INTRODUCTION

Resistance training is recognized as a powerful stimulus for skeletal muscle adaptation, driving increases in the mass and strength of muscle that are protective against age-related chronic diseases (1). Gains in muscle mass are underpinned by protein accretion and are accompanied by changes to the protein composition (i.e., proteome) of muscle that result in changes to muscle function, including speed of contraction and resistance to fatigue. Changes to the muscle proteome occur when the balance between synthesis and degradation of individual proteins changes (2). In response to resistance exercise, changes to the rates of synthesis and degradation are directed by intracellular mechanisms that integrate the mechanical signals with other information (e.g., energy balance, endocrine state, developmental stage, immune function) to appropriately allocate cellular resources to muscle growth (3). There is strong interest in optimizing the positive outcomes of muscle hypertrophy, fatigue resistance, and metabolism, to enhance athletic performance, prevent chronic disease, and mitigate age-related functional decline. Nevertheless, knowledge of the mechanisms of adaptation is incomplete, and this limits our ability to optimize the process of muscle adaptation to suit specific outcomes and populations.

Muscle hypertrophy (protein accretion) is a key objective of resistance training, and substantial research effort has been dedicated to optimizing muscle protein synthetic responses in humans (4). The fractional synthetic rate (FSR) of mixed myofibrillar proteins is known to double during the first 3-h period after a bout of resistance exercise (5). However, the magnitude of the synthetic response measured by short-term infusion of amino acid tracers greatly exceeds the gains in muscle mass accrued over weeks of resistance training, in part because muscle protein degradation is also elevated during the hours after resistance exercise (5). When

Correspondence: J. G. Burniston (j.burniston@ljmu.ac.uk).
Submitted 20 March 2025 / Revised 10 April 2025 / Accepted 13 October 2025

protein synthesis is measured over a time span of weeks with deuterium oxide (D_2O), resistance training is associated with an ~18.5% increase in FSR (6) that reflects the net contributions of synthesis and degradation and correlates positively with gains in muscle size. D_2O labeling can be readily combined with proteomic techniques to investigate the synthesis rate of individual muscle proteins (7) and has been used to study muscle responses to resistance exercise in humans (8, 9) and selective androgen receptor modulators in rats (10). In rat muscle, the FSRs of 34 proteins, including myofibrillar proteins and glycolytic enzymes, increase in a dose-dependent manner during the first week of treatment, and 70% (65 out of 94 proteins studied) of proteins exhibit positive correlations between the magnitude of increase in FSR during the first week and the gain in muscle mass after 28 days of selective androgen receptor modulator treatment (10).

The aforementioned correlative analyses between early protein FSR responses and subsequent gains in muscle mass cannot demonstrate the link between synthesis, degradation, and changes in abundance on a protein-by-protein basis. Instead, dynamic proteomic profiling, encompassing measurements of both the abundance and synthesis rate of individual proteins, is required (2). When studied with dynamic proteomic methods, the response of human muscle to resistance training (8) or high-intensity interval training (11) includes proteins that increase in FSR without exhibiting a change in abundance (i.e., turnover rate is increased) and proteins that decrease in abundance despite exhibiting an increase in FSR. These findings indicate co-occurring changes in protein degradation and highlight that the efficacy of resistance training protocols to accrue muscle mass cannot be assessed on the basis of the magnitude of the protein synthetic response alone.

In laboratory animals (12) and cell cultures (13), the Absolute Dynamic Profiling Technique for Proteomics (Proteo-ADPT) offers the opportunity to include measurements of total protein content and thereby report absolute rates (e.g., μg/day) of synthesis and degradation on a protein-by-protein basis. Using Proteo-ADPT, Hesketh et al. (12) showed that the transformation of rat fast-twitch muscle by chronic low-frequency stimulation involves approximately equal contributions from changes in protein degradation and synthesis. In some instances, changes in degradation rate primarily drive gains in protein abundance, whereas some decreases in protein abundance occur primarily via a decrease in synthesis (12). Chronic low-frequency stimulation is associated with a 50% reduction in muscle mass over 4 wk (12) concomitant with large metabolic adaptations and fast-to-slow fiber type shifts. By contrast, in the present study we investigated the role of changes in protein dynamics during the increase in muscle mass in response to unilateral programmed resistance training (PRT). Programmed cocontraction of rat lower limb muscles by electrical nerve stimulation in vivo leads to significant (~15%) gains in mass of the ankle dorsiflexor muscles during a 30-day experimental period (14, 15). In the present work, exercised and contralateral control muscles were studied during early (*days 0–10*), mid (*days 10–20*), and late (*days 20–30*) periods of adaptation. Our findings highlight that elevations in protein synthesis are significantly greater than the gains in muscle mass during the first 10 days of resistance training, and we discovered different temporal patterns of adaptation between ribosomal and mitochondrial proteins.

MATERIALS AND METHODS

Animals and Experimental Design

Experimental procedures were conducted under the auspices of the British Home Office Animals (Scientific Procedures) Act 1986 (License number: PA693D221). Three-month-old male Wistar rats (412 ± 69 g body wt; $n = 16$) were bred in-house in a conventional colony and housed in controlled conditions of 20°C and 45% relative humidity under a 12-h light (0600–1800) and 12-h dark cycle; water and food were available ad libitum. Animals were assigned to one of four groups ($n = 4$ in each), including a sham-operated control group and three experimental groups that received deuterium oxide (D_2O; Sigma-Aldrich, St. Louis, MO) for either 10-day, 20-day, or 30-day duration. D_2O labeling was initiated by an intraperitoneal bolus of 10 μL of 99% D_2O-saline/g body wt on the first day of resistance training and maintained by supplementing the animals' drinking water with 5% (vol/vol) D_2O, which was refreshed daily.

Unilateral programmed resistance training was used to simulate high-intensity resistance training with an implanted device. Electrical nerve stimulation intended to induce hypertrophy by loaded contractions of the tibialis anterior (TA) was conducted as described previously by our group (14). Electrical stimulators were implanted a week before the start of training. Buprenorphine (Temgesic; Indivior, Slough, UK) at a dose of 0.05 mg/kg body mass was administered preoperatively for analgesia, and surgery was performed with aseptic precautions. Anesthesia was induced with a gaseous mixture of 4% isoflurane in medical oxygen and was then adjusted to 1–2% isoflurane to maintain an adequate plane of surgical anesthesia. Electrodes were placed underneath the common peroneal nerve (cathode) and near to the tibial nerve (anode), to exploit the different activation thresholds for anodic and cathodic stimulation. The lower threshold of cathodic stimulation recruits all axons of the peroneal nerve so the dorsiflexors, including the TA, are maximally activated. An amplitude was set that provided sufficient additional activation of the plantar flexors via the tibial nerve to resist the action of the dorsiflexors so that the ankle joint angle did not decrease. Force produced by the stronger plantar flexor muscles was transmitted via the ankle and was used to achieve auxotonic contractions of the tibialis anterior. The 0-day time point represents the sham-operated control group that were implanted with inactive stimulators and then killed after a 1-wk recovery period. The remaining animals had the stimulation patterns implemented remotely 1 wk after the implant operation with the Mini-VStim-App installed on a standard Android-driven tablet computer (Xperia Tablet Z; Sony Corporation, Tokyo, Japan). The tablet computer connected via Bluetooth connection to a Mini-VStim programming device that communicated with the pulse generator via a radio frequency link. Once programmed, the stimulator operated autonomously to provide

daily exercise sessions in one limb, and the animals were housed in their normal cages and monitored daily.

The stimulation pattern consisted of a daily "warm-up" phase of 40 twitches at 4 Hz over a duration of 10 s, which immediately preceded the resistance training program. The resistance training stimulus used five sets of 10 repetitions. Each repetition consisted of a 2-s fused near-maximal tetanic contraction at a stimulation frequency of 100 Hz. Two-second recovery was allowed between repetitions, and 2.5 min of rest was allowed between sets. One hour after daily stimulation on *days 10*, *20*, and *30*, groups of $n = 4$ animals were killed humanely in a rising concentration of CO_2 followed by cervical dislocation. Plasma samples were obtained by cardiac puncture immediately after death, and tibialis anterior from the left stimulated (Stim) and the right nonstimulated (Ctrl) limb were isolated. Each muscle was cleaned of fat and connective tissue and then weighed before being frozen in liquid nitrogen and stored at −80°C pending further analysis.

Muscle Processing

Muscles were fractionated into myofibrillar and soluble fractions according to Hesketh et al. (12). Samples were pulverized under liquid nitrogen with a mortar and pestle. An analytical balance was used to accurately record an aliquot (~100 mg) of muscle powder, which was then mechanically homogenized on ice in 10 volumes of 1% Triton X-100, 50 mM Tris pH 7.4 including phosphatase inhibitor and complete protease inhibitor cocktails (Roche, Indianapolis, IN). Homogenates were incubated on ice for 15 min and then centrifuged at 1,000 *g*, 4°C for 5 min. Supernatants containing soluble proteins were decanted and stored on ice while the myofibrillar pellet was washed by resuspension in 0.5 mL of homogenization buffer and then centrifuged at 1,000 *g*, 4°C for 5 min. The washed myofibrillar pellet was solubilized in 10 volumes of 7 M urea, 2 M thiourea, 4% CHAPS, 30 mM Tris, pH 8.5 and cleared by centrifugation at 12,000 *g*, 4°C for 45 min. Protein concentrations of each myofibrillar and soluble protein sample were measured by the Bradford assay (Sigma-Aldrich, Poole, United Kingdom). The protein concentrations of experimental samples were interpolated from bovine serum albumin standards (0.125–1.0 mg/mL range) by linear regression. The total protein content (mg) of each muscle was calculated by multiplying muscle wet weight (WW; mg) by the yield of protein extracted from an aliquot of muscle powder (MP; mg) divided by the protein concentration (PC; mg/mL) and homogenate volume (HV; mL) of the myofibrillar and soluble protein fractions (*Eq. 1*).

$$\text{Muscle protein content} = \left(\frac{\text{MP}}{\text{PC} \cdot \text{HV}}\right) \cdot \text{WW} \qquad (1)$$

Muscle proteins were processed for mass spectrometry by tryptic digestion according to the filter-aided sample preparation method (16). Lysates containing 100 μg of protein were precipitated in 5 volumes of acetone at −20°C for 1 h. After centrifugation (5,000 *g*, 5 min), acetone was decanted and the protein pellets were air-dried and then resuspended in 200 μL of UA buffer (8 M urea, 100 mM Tris, pH 8.5). Samples were incubated at 37°C for 15 min in UA buffer with 100 mM dithiothreitol followed by 20 min at 4°C in UA buffer containing 50 mM iodoacetamide (protected from light). Samples were washed twice with 100 μL of UA buffer and transferred to 50 mM ammonium hydrogen bicarbonate. Sequencing-grade trypsin (Promega; Madison, WI) in 50 mM ammonium hydrogen bicarbonate was added at an enzyme-to-protein ratio of 1:50, and the samples were digested overnight at 37°C. To terminate digestion, peptides were collected in 50 mM ammonium hydrogen bicarbonate and trifluoracetic acid was added to a final concentration of 0.2% (vol/vol). Aliquots containing 4 μg of peptides were desalted with C_{18} Zip-tips (Millipore, Billerica, MA) and eluted in 50:50 acetonitrile-0.1% trifluoracetic acid. Peptide solutions were dried by vacuum centrifugation for 25 min at 60°C, and peptides were resuspended in 0.1% formic acid spiked with 10 fmol/μL yeast alcohol dehydrogenase 1 (Waters Corp.) in preparation for liquid chromatography-tandem mass spectrometry analysis (17).

Liquid Chromatography-Tandem Mass Spectrometry

Peptide mixtures were analyzed with an Ultimate 3000 Rapid Separation Liquid Chromatography nano system (Thermo Scientific) coupled to a Q-Exactive orbitrap mass spectrometer (Thermo Scientific). Samples were loaded, via μl Pick-up injection, onto the trapping column (Thermo Scientific, PepMap100, 5 μm C_{18}, 300 μm × 5 mm) in 0.1% (vol/vol) trifluoracetic acid and 2% (vol/vol) acetonitrile at a flow rate of 25 μL/min for 1 min. Samples were resolved on a 500-mm analytical column (Easy-Spray C_{18} 75 μm, 2-μm column) and peptides eluted with a linear gradient from 97.5% A (0.1% formic acid):2.5% B (79.9% acetonitrile, 20% water, 0.1% formic acid) to 50% A:50% B over 150 min at a flow rate of 300 nL/min. Data-dependent selection of the top 10 precursors selected from a mass range of m/z 300–1,600 was used for data acquisition, which consisted of a 70,000-resolution (at m/z 200) full-scan MS scan (automatic gain control set to $3e^{06}$ ions with a maximum fill time of 240 ms). MS/MS data were acquired by quadrupole ion selection with a 3.0 m/z window, higher-energy collisional dissociation fragmentation with a normalized collision energy of 30, and in the orbitrap analyzer at 17,500-resolution at m/z 200 (automatic gain control set to $5e^{04}$ ions with a maximum fill time of 80 ms). To avoid repeated selection of the same peptides for MS/MS, a dynamic exclusion window of 30 s was applied.

Label-Free Quantification of Protein Abundances

Progenesis Quantitative Informatics for Proteomics (QI-P; Nonlinear Dynamics, Waters Corp., Newcastle, UK) was used for label-free quantitation (LFQ), consistent with previous studies (8, 11, 12). MS data were normalized by intersample abundance ratio, and relative protein abundances were calculated using nonconflicting peptides only. MS/MS spectra were exported in Mascot generic format and searched against the Swiss-Prot database (2022_08) restricted to "Rattus" (8,071 sequences), using a locally implemented Mascot server (v.2.8; www.matrixscience.com) with automatic target-decoy search. The enzyme specificity was trypsin with two allowed missed cleavages, carbamidomethylation of cysteine (fixed modification) and oxidation of methionine (variable modification). m/z error tolerances of 10 ppm for peptide ions and 20 ppm for fragment ion spectra were used. The Mascot output (xml format) restricted

to nonhomologous protein identifications was recombined with MS profile data in Progenesis. Protein abundance data were calculated using only unique peptides with high confidence [<1% false discovery rate (FDR)] identification scores. The mass spectrometry proteomics data have been deposited to the ProteomeXchange Consortium via the PRIDE partner repository with the dataset identifier PXD060879 and 10.6019/PXD060879.

Measurement of Body Water D_2O Enrichment

Body water enrichment of deuterium oxide (D_2O) was measured in plasma samples against external standards constructed by adding D_2O to phosphate-buffered saline over the range from 0.0 to 5.0% in 0.5% increments. D_2O enrichment of aqueous solutions was determined by gas chromatography-mass spectrometry after exchange with acetone (18). Samples were centrifuged at 12,000 *g*, 4°C for 10 min, and 20 μL of plasma supernatant or standard was reacted overnight at room temperature with 2 μL of 10 M NaOH and 4 μl of 5% (vol/vol) acetone in acetonitrile. Acetone was extracted into 500 μL of chloroform, and water was captured with 0.5 g of Na_2SO_4. A 200-μL aliquot of chloroform was transferred to an autosampler vial, and samples and standards were analyzed in triplicate with an Agilent 5973 N mass selective detector coupled to an Agilent 6890 gas chromatography system (Agilent Technologies, Santa Clara, CA). A CD624-GC column (30 m × 0.53 mm × 3 μm) was used in all analyses. Samples (1 μL) were injected with an Agilent 7683 autosampler. The temperature program began at 50°C, increased by 30°C/min to 150°C, and was held for 1 min. The split ratio was 50:1 with a helium flow of 1.5 mL/min. Acetone eluted at ~3 min. The mass spectrometer was operated in the electron impact mode (70 eV), and selective ion monitoring of *m*/*z* 58 and 59 was performed with a 10 ms/ion dwell time. Percent D_2O enrichment of experimental samples was calculated by interpolation from the standard curve by linear regression.

Absolute Dynamic Profiling Technique for Proteomics

The Absolute Dynamic Profiling Technique for Proteomics (Proteo-ADPT) was conducted by calculating absolute protein abundance and synthesis rates on a protein-by-protein basis, originally described in Hesketh et al. (12). Relative protein abundances (fmol/μg protein on column) measured by label-free quantification were converted to absolute (μg) values with *Eq. 2*.

$$\mathrm{P} = \mathrm{ABD_{Rel}} \cdot \mathrm{MW} \cdot \text{muscle protein content} \tag{2}$$

That is, the absolute abundance (P; μg/muscle) of each protein was calculated from the relative abundance (ABD_{rel}; fmol/μg total protein) measured by LFQ multiplied by the molecular weight (MW) of the protein (referenced from the UniProt Knowledgebase) and the total protein content (mg) of the muscle (derived in *Eq. 1*).

Mass isotopomer abundance data were extracted from MS spectra with Progenesis Quantitative Informatics (Non-Linear Dynamics, Newcastle, UK). Consistent with previous work (8, 12, 19), the abundances of peptide mass isotopomers were collected over the entire chromatographic peak for each proteotypic peptide that was used for label-free quantitation of protein abundances. Mass isotopomer information was processed with in-house scripts written in Python (version 3.12.4). The incorporation of deuterium into newly synthesized protein was assessed by measuring the increase in the relative isotopomer abundance (RIA) of the m_1 mass isotopomer relative to the sum of the m_0 and m_1 mass isotopomers (*Eq. 3*), which exhibits rise-to-plateau kinetics of an exponential regression (20) as a consequence of biosynthetic labeling of proteins in vivo.

$$\mathrm{RIA} = \frac{m_1}{m_0 + m_1} \tag{3}$$

The plateau in RIA ($RIA_{plateau}$) of each peptide was derived (*Eq. 4*) from the total number (*N*) of ^2H exchangeable H—C bonds in each peptide, which was referenced from standard tables (21) and the difference in the D-to-H ratio ($^2H/^1H$) between the natural environment (DH_{nat}) and the experimental environment (DH_{exp}) based on the molar percent enrichment of deuterium in the precursor pool, according to previous work (22).

$$\mathrm{RIA_{plateau}} = 1 - \left(\frac{1}{\left(\frac{1}{1-\mathrm{RIA}(t_0)} \right) + N(\mathrm{DH_{exp}} - \mathrm{DH_{nat}})} \right) \tag{4}$$

The rate constant of protein degradation (k_{deg}) was calculated (*Eq. 5*) between the beginning (t_0) and end (t_1) of each 10-day labeling period. Calculations for exponential regression (rise to plateau) kinetics reported previously (22) were used, and k_{deg} data were adjusted for differences in protein abundance (*P*) between the beginning (t_0) and end (t_1) of each labeling period.

$$k_{\mathrm{deg}} = -\frac{1}{t - t_0} \cdot \ln\left(1 - \frac{\mathrm{RIA}(t_1) - \mathrm{RIA}(t_0)}{\mathrm{RIA_{plateau}} - \mathrm{RIA}(t_0)}\right) \cdot \frac{P(t)}{P(t_0)} \tag{5}$$

Absolute synthesis rates (ASRs) were derived (*Eq. 6*) by multiplying peptide K_{deg} by the absolute abundance (e.g., μg protein/muscle) of the protein at the end of the labeling period *P*(*t*).

$$\mathrm{ASR} = P(t) \cdot k_{\mathrm{deg}} \tag{6}$$

Absolute degradation rates (ADRs) were derived (*Eq. 7*) by subtracting the rate of change in abundance from the absolute synthesis rate.

$$\mathrm{ADR} = \mathrm{ASR} - \left(\frac{P(t) - P(t_0)}{t - t_0} \right) \tag{7}$$

Statistical and Bioinformatic Analysis

Unless stated otherwise, data are presented as mean ± standard deviation and statistical analyses were conducted in R (version 4.3.1). Muscle wet weight and protein content were normalized to animal body weight and analyzed by mixed analysis of variance (ANOVA). Where appropriate (i.e., non-omics data), significant ($P < 0.05$) interactions were further investigated by post hoc pairwise comparisons of estimated marginal means with Bonferroni adjustment.

Proteomic data were filtered to exclude proteins that were not quantified in all conditions (Stim and Ctrl) at all experimental time points (0, 10, 20, and 30 days) in all biological

replicates ($n = 4$, in each group), i.e., proteins with missing values were removed and no data were imputed. Two-factor mixed ANOVA was used to identify significant interactions between condition (PRT stimulated vs. contralateral control) and time (experimental time points: 0, 10, 20, and 30 days). In addition, within-subject ANOVA was used to investigate differences between PRT stimulated and contralateral control muscle at each experimental time point or period. Type I error was controlled with the calculation of false discovery rates (q values) and Benjamini–Hochberg-adjusted P values (BH-adj P) with the "qvalue" package (R/Bioconductor) (23).

Relationships between changes in protein abundances and/or absolute synthesis rates were assessed by linear regression at single experimental time points or multiple linear regression across multiple experimental time points. Regression models predicting changes in absolute protein abundance from absolute synthesis rate data were constructed using the $\log_2$ fold difference between stimulated and contralateral control muscles at each experimental time point.

Proteins that exhibited statistically significant (BH-adj $P < 0.05$) interactions (condition × time) in abundance were submitted to bioinformatic analyses to further explore differences in the temporal profile of protein abundance changes. To enable exploration of temporal profiles of individual protein synthesis rates, unsupervised clustering was conducted across all protein-specific absolute synthesis rate (ASR) data to identify patterns and networks of proteins with similar synthesis rate dynamics across the 30-day experimental period. Temporal profiles (using $\log_2$ fold difference Stim/Ctrl at *days 0*, *10*, *20*, and *30*) were normalized with the "standardise()" function within the Mfuzz R package (24) and submitted to soft clustering analysis using the fuzzy *c*-means clustering algorithm. The optimal number of clusters was determined by inspection of scree plots and qualitative iterative assessment of cluster membership profiles. The minimum membership value for inclusion into a cluster was set at 0.5 throughout. Proteins exhibiting significant differences between Stim and Ctrl across the time course and subsequent temporal clusters were further investigated by bibliometric mining in the Search Tool for the Retrieval of INteracting Genes/proteins (STRING, version 12), using the evidence of interaction sources of bibliometric text mining, experimental verified protein-protein interaction data, gene ontology databases, and coexpression data with the minimum required interaction score set at 0.4 (medium confidence). Protein-protein interaction networks and functional enrichment analyses were conducted with the STRINGdb package in R (version 2.12.1) (25) and corrected against the experiment-specific background consisting of all proteins that were included in statistical analysis. Protein-protein interaction networks were transferred via the RCy4 R package (version 1) and visualized with Cytoscape version 3.9.1 (26).

RESULTS

Daily PRT Increases TA Wet Weight and Protein Content

At the onset (*day 0*) of the experiment there was no difference in either tibialis anterior wet weight or protein content between the left (sham operated) and right (contralateral control) limbs. Programmed resistance training significantly ($P < 0.001$) increased the wet weight (Fig. 1*B*) and total protein content (Fig. 1*C*) of the tibialis anterior after 10-day stimulation ($+15.52 \pm 7.79\%$ and $+30.48 \pm 8.56\%$, respectively), and this gain was sustained across the 20-day ($+19.48 \pm 3.22\%$ and $+50.21 \pm 12.68\%$, respectively) and 30-day ($+18.13 \pm 7.93\%$ and $+40.02 \pm 10.99\%$) time points, respectively. The changes in muscle wet weight correlated closely (Pearson correlation coefficient = 0.87, $P = 1.156e^{-05}$) with changes in muscle protein accretion (Fig. 1*D*), indicating that the increases in muscle wet weight were not due to edema that may accompany muscle damage.

The Proteome of Contralateral (Nonstimulated) Control Muscle Was Unaffected by Programmed Resistance Training

Our proteomic analysis confidently identified and quantified the abundance of 1,083 proteins in rat tibialis anterior. Before statistical analyses, protein abundance data were stringently filtered to exclude proteins that were not quantified in all stimulated and control muscles ($n = 4$, in each group) across all experimental time points (*days 0*, *10*, *20*, and *30*). After filtering, 658 proteins were quantified in all 32 biological samples. Protein abundances (expressed as mass of protein in each tibialis anterior muscle) spanned from 0.49 ± 0.32 ng (Histone H1.1) to 28.514 ± 3.846 mg (Myosin heavy chain 4), and the top 10 most abundant proteins accounted for >50% (~53 mg) of total protein content (92 mg) in control muscles collected on *day 0* (Fig. 2*A*).

At the onset of the experiment (*day 0* samples), there was no significant difference in the abundance of any protein between the sham-operated and contralateral control muscles. The protein abundance profile of sham-operated and contralateral control muscle was highly correlated ($r = 0.999$) (Fig. 2*B*), and the median coefficient of variation in protein abundance among samples was 4.6% (1st quartile = 2.04% and 3rd quartile = 6.64%). Protein abundances were unchanging across contralateral control muscles collected from independent animals across the 30-day experimental period. Ordinary least squares regression indicated a strong linear relationship between the abundance of proteins in control muscles at onset of the experiment (*day 0*) compared to *day 10* ($r^2 = 0.995$), *day 20* ($r^2 = 0.989$), and *day 30* ($r^2 = 0.991$) (Fig. 2*C*). We are confident that these findings demonstrate a high level of consistency across the independent groups of control muscles during the 30-day experimental period and that the control muscles were little affected by daily stimulation in the exercised limb.

Ribosomal Proteins Respond Early to Programmed Resistance Training

Programmed resistance exercise resulted in robust (BH-adj $P < 0.05$; condition × time interaction) changes in the abundance of 187 proteins across the 30-day training period. Unsupervised soft clustering performed on the 187 significant proteins highlighted two prominent temporal patterns of change among the proteins that responded to programmed resistance exercise (Fig. 2*D*). Proteins in Abundance Cluster 1 (ABD_Cluster_1; 74 in total) exhibited increases in absolute abundance after the first 10 days of

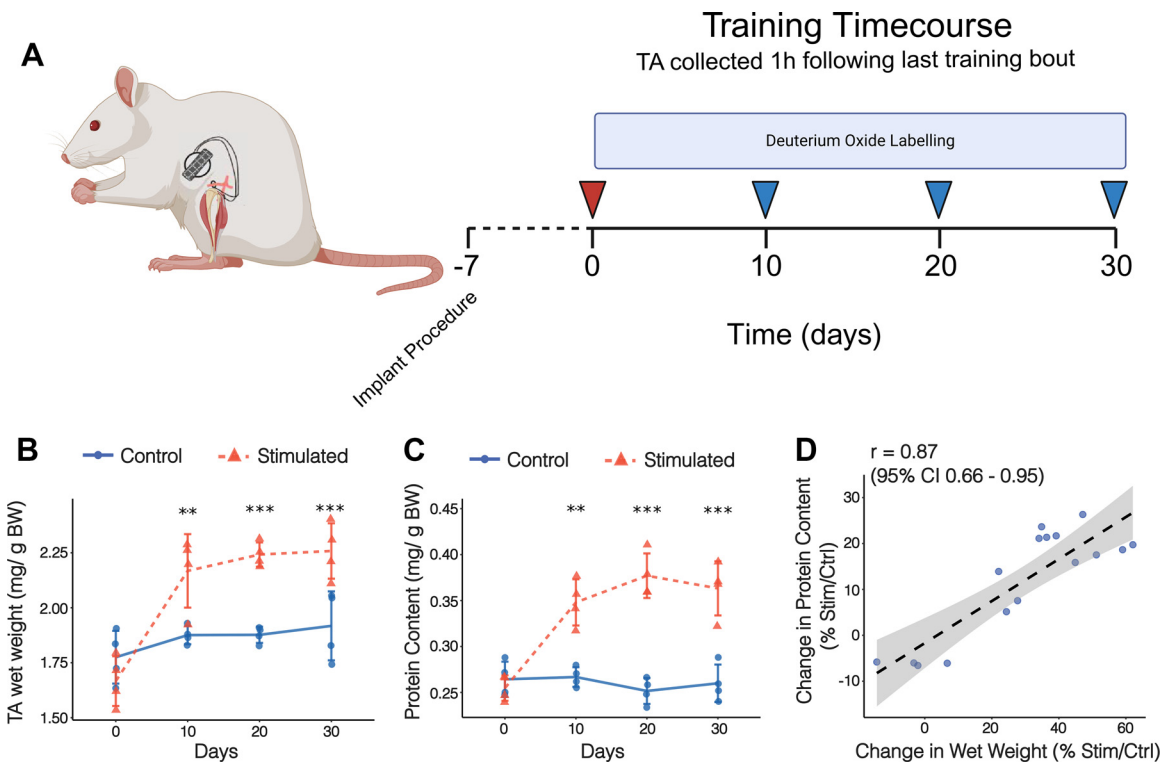

Figure 1. Daily programmed resistance training (PRT) increases tibialis anterior (TA) wet weight and protein content. *A*: PRT in vivo was achieved with implantable pulse generators placed in the abdomen with electrodes routed subcutaneously to the left limb. Within-animal unilateral PRT model ($n = 4$ per time point) uses loaded contractions of the TA (resisted by the plantarflexors) in the left hindlimb while the right remains unstimulated. Rats were stimulated daily during the early phase of the light period. Control and sham-operated control TA muscles were collected (red arrow) before the initiation of deuterium oxide (D_2O) labeling on *day 0*. D_2O labeling was initiated at *day 0* and maintained by administration of D_2O in the drinking water available ad libitum. Stimulated (Stim) and control (Ctrl) limb muscles were collected 1 h after the last training bout following 10, 20, or 30 days of daily training (blue arrows). PRT consisted of 5 sets of 10 repetitions of 2 s on, 2 s off tetanic contractions at 100 Hz with 2.5 min of rest between sets. *B*: time course changes in TA mass [TA wet weight relative to body weight (BW); mg/g] of the stimulated and control limbs across the experimental time course. *C*: protein content (relative to BW; mg/g) measured by Bradford assay. Data are presented as means ± SD with individual data points plotted for each muscle analyzed. Data were analyzed with a 2-way ANOVA. Significant interactions (Condition × Time) were investigated by pairwise comparisons with Bonferroni adjustment. $^{**}P \leq 0.01$, $^{***}P \leq 0.001$. *D*: correlation analysis of changes in TA wet weight and protein content. Data points represent percent change (Stim/Ctrl) from $n = 4$ biological replicates across 0, 10, 20, and 30 days. CI, confidence interval.

training that then plateaued after 20 days or 30 days of resistance exercise (Fig. 2*D*). Biological Processes including posttranscriptional regulation and translation of mRNA (Fig. 3, *A* and *B*) were significantly enriched among proteins in ABD_Cluster_1, which included 18 ribosomal proteins encompassing 10 large (60S) and 8 small (40S) ribosomal subunits. Eukaryotic initiation factors eIF3A and eIF2G were also included within ABD_Cluster_1 alongside the eukaryotic translation elongation factor eEF1D and the peptide chain release factor ERF1. In addition, ABD_Cluster_1 contained a network of proteins associated with skeletal muscle development and organization including four tubulin proteins (TBA1B, TBA4A, TBB4A, and TBB5), dynactin subunit 1 and 2, Nexilin, WD repeat-containing protein 1, Alpha-crystallin B chain, Vimentin, Prelamin-A/C, Tropomodulin-1, and five nontypical myosin isoforms (MY18A, MYH11, MYH8, MYH9, and MYO1C).

In all, our analysis quantified the abundance of 57 out of the 80 annotated subunits of the ribosome, including 30 subunits of the 60S large ribosome and 27 subunits of the 40S small ribosome. Changes in the summed abundance of ribosomal proteins (r-proteins) in response to programmed resistance training mirrored the accretion of total muscle protein (Fig. 3, *C* and *D*), and changes in the total content of the 40S and 60S subunits exhibited a significant ($P = 0.047$ and 0.0097, respectively) interaction between condition (stimulated vs. contralateral control) and experimental time point (*days 0*, *10*, *20*, and *30*). Post hoc analysis indicated that after 10 or more days of programmed resistance training the total r-protein content of the 60S subunit was 84% greater ($P = 0.01$) compared to the contralateral control, and the total abundance of 40S subunits tended ($P = 0.06$) to be 76% greater compared to control after 20 days of training (Fig. 3, *C* and *D*).

Mitochondrial Protein Response Occurs after Ribosomal Protein Response

Proteins in ABD_Cluster_2 exhibited more gradual rises (compared to ABD_Cluster_1) in abundance and did not exhibit statistically relevant differences between the stimulated and control conditions until after 20 days and 30 days of training (Fig. 2*D*). ABD_Cluster_2 included 114 mitochondrial proteins (from 162 proteins assigned to Cluster 2) and was significantly enriched (FDR < 0.001) in a collection of GO terms associated with mitochondria and cellular respiration (Fig. 4 *A* and *B*) including 23 proteins

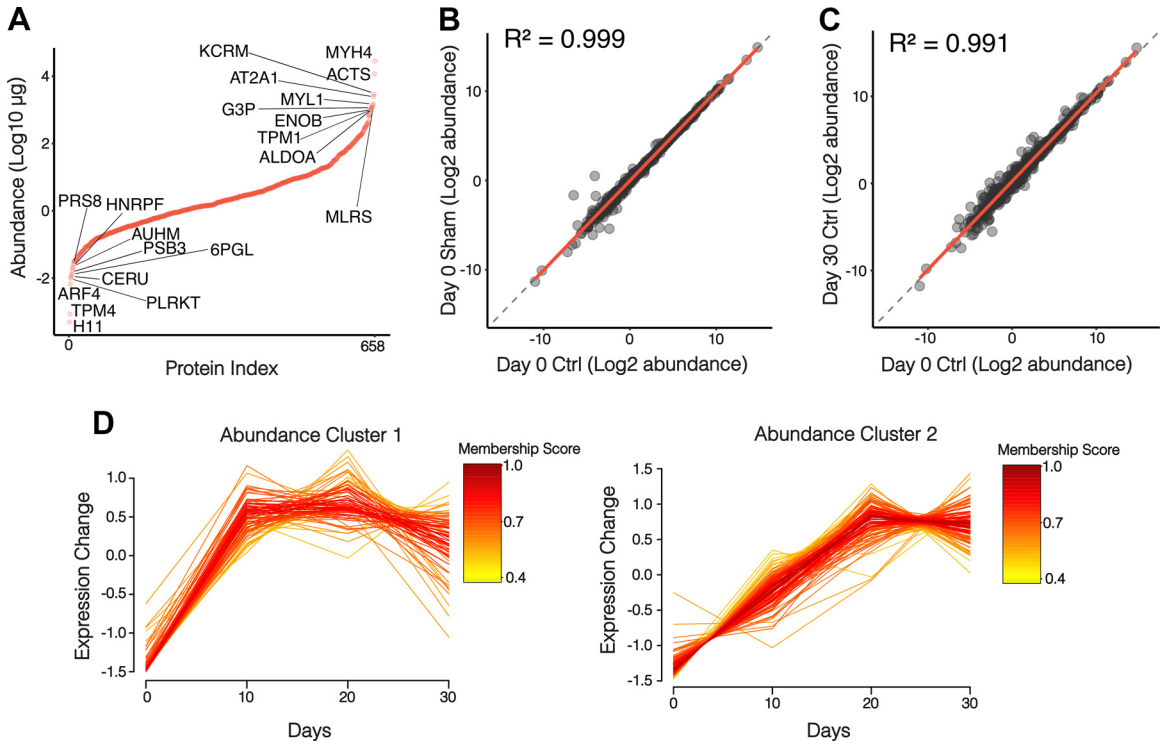

Figure 2. Absolute quantification of muscle proteins in rat tibialis anterior (TA). *A*: distribution plot of $\log_{10}$ transformed absolute protein abundances (µg of protein) for 658 proteins successfully quantified across all 32 muscle samples. Data points represent mean abundance from control (Ctrl) TA at the onset of the experiment ($n = 4$). *B*: ordinary least squares (OLS) regression analysis (R^2) of absolute abundance (µg) of $n = 658$ proteins quantified in TA of $n = 4$ sham-operated and contralateral Ctrl limbs at the beginning (*day 0*) of the experimental period. *C*: OLS (R^2) of protein abundances ($n = 658$) quantified in Ctrl TA at the beginning (*day 0*) and end (*day 30*) of the experimental period ($n = 4$, biological replicates). *D*: absolute protein abundances (µg of protein) were analyzed by 2-way ANOVA. Proteins exhibiting a significant [Benjamini–Hochberg-adjusted (BH-adj) P value ≤ 0.05] interaction (Time × Condition) were further investigated by soft clustering analysis. Temporal profiles [$\log_2$ transformed stimulated (Stim)/Ctrl at each time point] of proteins exhibiting significant interactions were clustered with fuzzy *c*-means clustering algorithm with the Mfuzz R package. The minimum membership value for inclusion into a cluster was set at 0.5. Data reported from $n = 4$ biological replicates per time point (0, 10, 20, and 30 days) and condition (Stim and Ctrl).

associated with oxidative phosphorylation, comprising nine respiratory Complex I subunits and six ATP synthase subunits. The GO Biological Processes "Mitochondrion Organization" was significantly enriched (FDR = 0.01; 23 proteins) within ABD_Cluster_2 and included key regulators of mitochondrial quality control (e.g., VDAC1, VDAC2, VDAC3, FIS1, SAM50, SODM, PHB, and CH60). ABD_Cluster_2 was also significantly enriched with proteins associated with the KEGG pathway "TCA Cycle" (FDR = 0.01; 13 proteins), and ABD_Cluster_2 also contained the mitochondrial elongation factor TU and eIF5A1 (Fig. 4*A*).

The mitochondrial content of muscles was estimated by aggregating the absolute abundance (i.e., mg of protein per muscle) of proteins annotated to the GO Cellular Component "Mitochondrion." There was a significant ($P = 0.041$) interaction (2-way ANOVA of condition × time) in total mitochondrial protein content (Fig. 4*C*), and post hoc analysis revealed that mitochondrial protein content was greater ($P = 0.037$) in stimulated muscles after 30 days of resistance training.

Absolute Quantification of Proteome Dynamics

Proteo-ADPT was conducted on a subset of proteins that had high-quality peptide mass isotopomer profiles. Deuterium oxide consumption resulted in a body water (i.e., precursor) enrichment of 3.29 ± 0.14% ($n = 16$ animals), and, in total, the rates of synthesis of 585 proteins were quantified. After exclusion of missing values, the absolute and fractional synthesis rate [ASR (ng/day) and FSR (%/day), respectively] of 215 proteins were quantified in all samples ($n = 4$ stimulated and $n = 4$ contralateral control) across the early (0–10 days), mid (10–20 days), and later (20–30 days) measurement periods. Proteins included in the Proteo-ADPT analysis were among the most abundant in tibialis anterior and shared gene ontology terms including the biological processes "Metabolic Process" (159 proteins) and "Cellular Respiration" (46 proteins) and cellular components "Mitochondrion" (89 proteins) and "Myofibril" (35 proteins). In sum, the 215 proteins included in the Proteo-ADPT analysis represented ~70% of total muscle protein content.

Based on analysis of these 215 proteins, in control muscles the total amount of new protein synthesized averaged 2.61 ± 1.63 mg/day during the experimental period, which equates to an average mixed-protein FSR of 4.26 ± 2.17%/day. Two-way mixed ANOVA did not identify significant (NS; $P > 0.14$) effects of condition (stimulated vs. contralateral control) or interactions between condition and measurement period (0–10 days, 10–20 days, or 20–30 days) in either total ASR or mixed-protein FSR. Mixed-protein FSR was ~1.63-fold greater in stimulated (5.17 ± 1.48%/day) than in control (2.91 ± 0.68%/day) muscle during

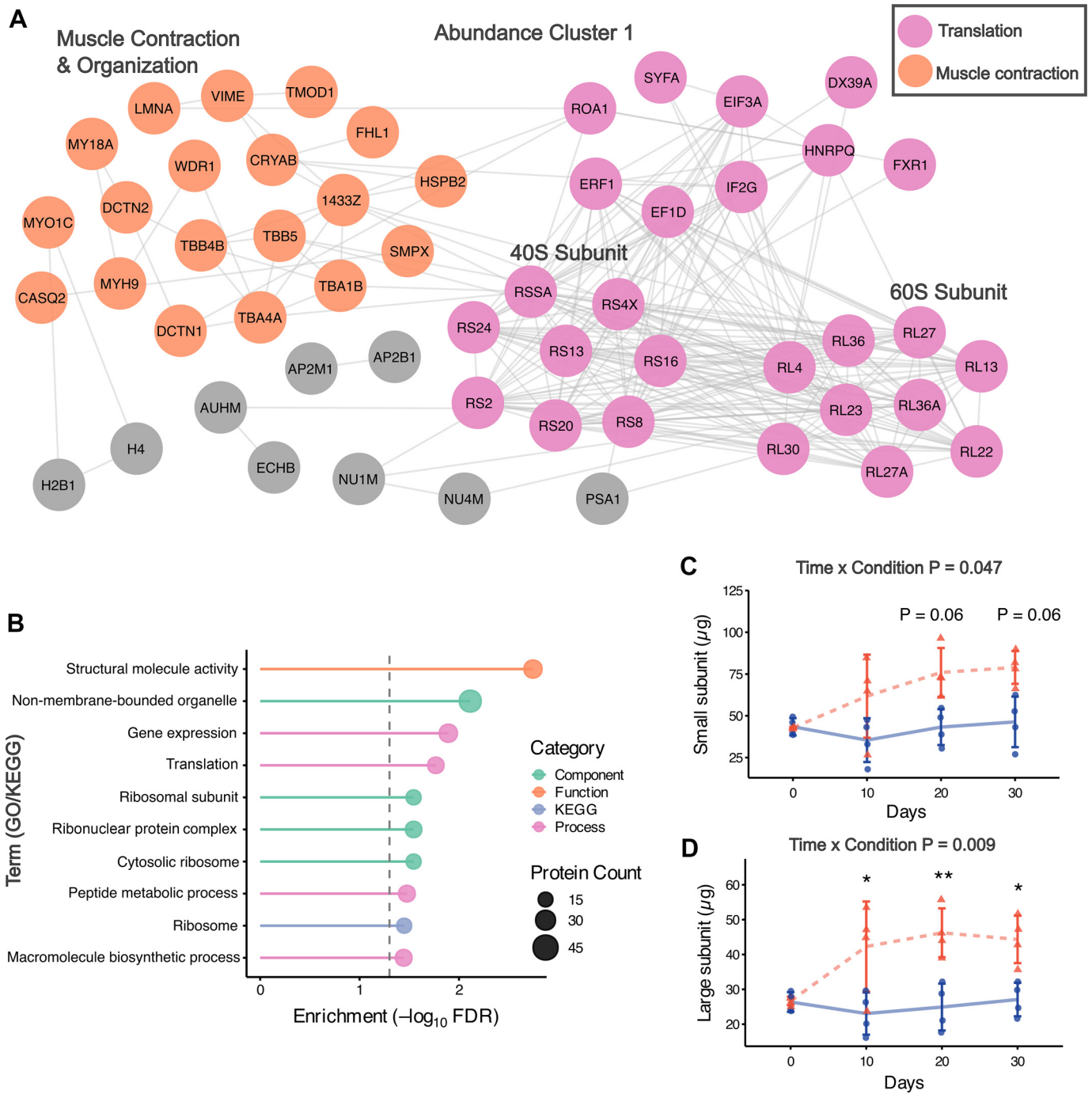

Figure 3. Ribosomal protein accretion occurs during early adaptation to resistance training. Bioinformatic analysis of time course clustering profiles identified in Fig. 2. *A* and *B* represent proteins included in Abundance Cluster 1, where *A* visualizes the Search Tool for the Retrieval of INteracting Genes/proteins (STRING) protein interaction network for proteins belonging to abundance cluster 1. Colored nodes represent proteins in Cluster 1 associated with muscle contraction and organization (orange) and protein translation (pink), including labeling of subnetworks of proteins associated with small (40S) and large (60S) ribosomal subunit. *B*: bubble plot represents significantly enriched [false discovery rate (FDR) < 0.05] Gene Ontology (GO) and KEGG pathway terms for proteins included in Abundance Cluster 1. *C* and *D*: time course changes in total ribosomal protein content (μg) of the "small" 40S (*C*) and "large" 60S (*D*) subunits. Data in *C* and *D* are presented as means ± SD and analyzed by a 2-way ANOVA. Significant interactions (Condition × Time) were investigated by pairwise comparisons with Bonferroni adjustment. $^{*}P \leq 0.05$, $^{**}P \leq 0.01$. Data reported from $n = 4$ biological replicates per time point (0, 10, 20, and 30 days) and condition [stimulated (Stim) and control (Ctrl)].

the early (0–10 days) response to programmed resistance training (Fig. 5, *A* and *B*), which equates to a nonsignificant rise of ~1.4 mg protein synthesized/day in stimulated (3.25 ± 1.78 mg/day) compared to control (1.86 ± 0.43 mg/day) muscle.

Translational efficiency (μg protein synthesized per μg r-protein content) was assessed by comparing the total ASR (mg/day protein synthesis) relative to r-protein content of each muscle. Translational efficiency (μg ASR/μg r-protein) in exercised muscle during the early (31.53 ± 10),

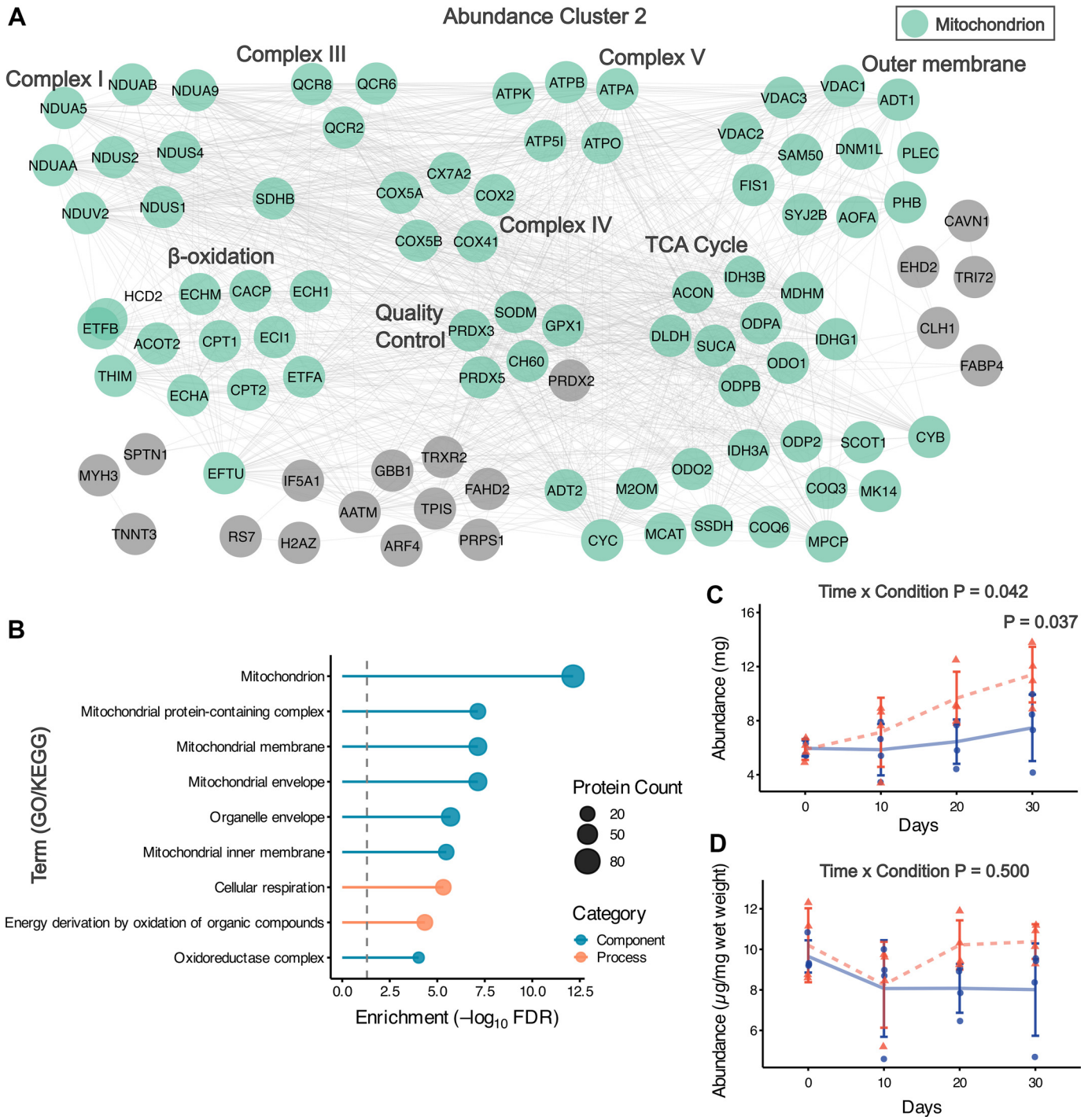

Figure 4. Mitochondrial protein accretion occurs later in the adaptation to resistance training. *A*: Search Tool for the Retrieval of INteracting Genes/proteins (STRING) protein interaction network for proteins displaying significant belonging to abundance cluster 2 reported in Fig. 2. Green-colored nodes represent proteins in Abundance Cluster 2 associated with the GO cellular component "Mitochondrion" alongside manual annotation of key subnetworks of mitochondrial proteins included within abundance cluster 2. *B*: bubble plot represents top 10 significantly enriched [false discovery rate (FDR) < 0.05] Gene Ontology (GO) terms for proteins included in Cluster 2. *C* and *D*: time course changes in total mitochondrial protein content expressed in absolute units (mg protein) (C) and relative to tibialis anterior (TA) wet weight (mg protein/mg) (*D*). Data in *C* and *D* are presented as means ± SD and analyzed by a 2-way ANOVA. Significant interactions (Condition × Time) were investigated by pairwise comparisons with Bonferroni adjustment. Data reported from $n = 4$ biological replicates per time point (0, 10, 20, and 30 days) and condition [stimulated (Stim) and control (Ctrl)].

mid (39.38 ± 17.75), or late (19.55 ± 5.87) experimental periods was not different from values in control muscle (Fig. 5*C*) during the early (29.71 ± 1.37), mid (45.04 ± 28.09), or late (38.09 ± 16.10) experimental periods.

Protein synthesis outweighed protein accretion during the early (0–10 days) adaptive response to programmed resistance training (Fig. 5*D*). There was a strong relationship ($r^2 = 0.725$) between the changes in ASR and the changes in

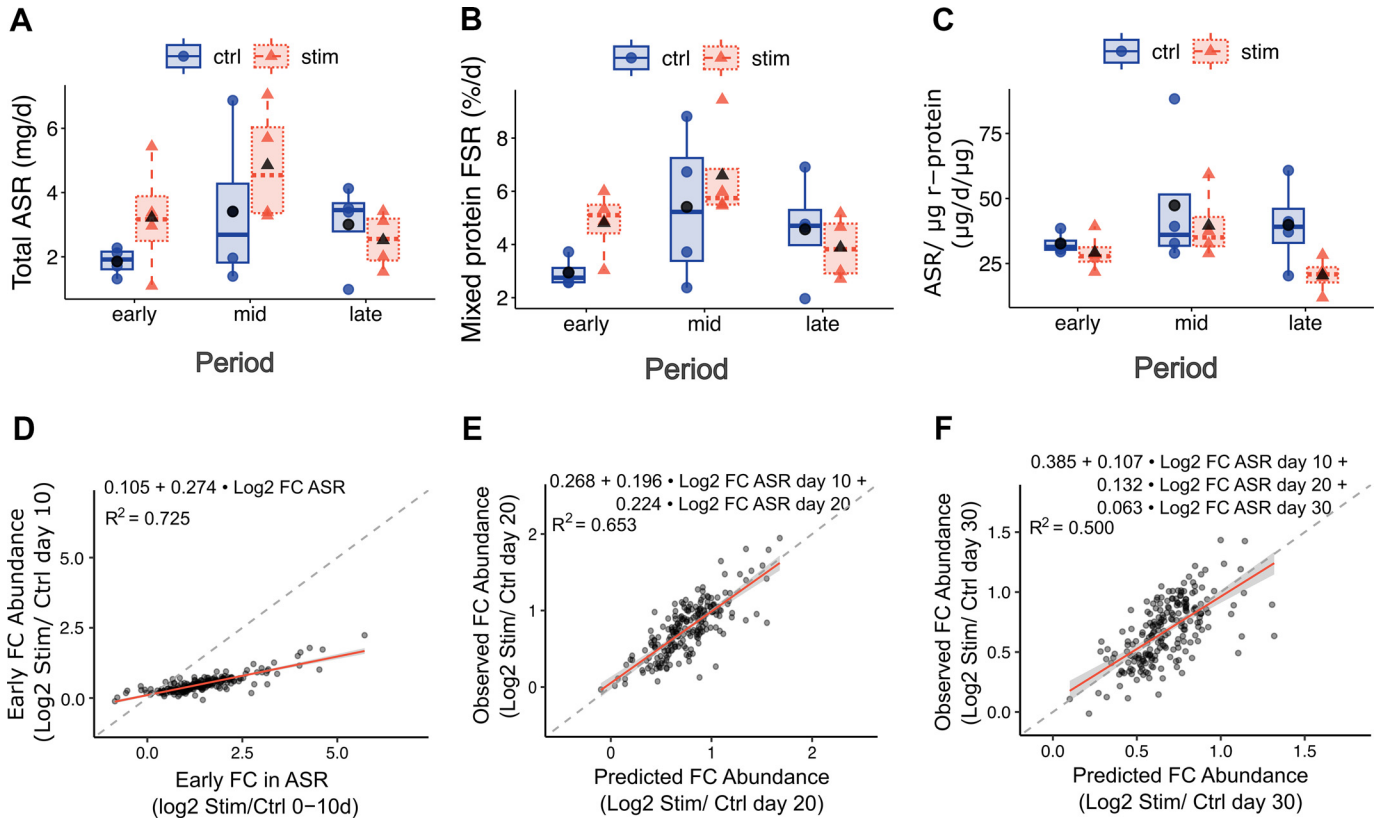

Figure 5. Absolute quantification of protein synthesis rates during programmed resistance training (PRT). *A*: boxplots of total muscle protein synthesis rates [sum of individual absolute synthesis rates (ASRs), expressed in mg/d] quantified from 216 protein-specific synthesis rates quantified across all measurement periods across the 30 day period of PRT. *B*: mixed-protein synthesis reported as fractional synthesis rates (FSRs; %/day) calculated from median FSR of 216 protein-specific synthesis rates quantified across all measurement periods across the 30-day period of PRT. *C*: estimates of translational efficiency in stimulated and control muscles across the time course of PRT expressed. Translational efficiency is reported as total muscle protein synthesis (total ASR; µg/day) relative to total ribosomal protein (r-protein) content (µg) to report total protein synthesized per day per µg of r-protein. Data analyzed with a 2-way ANOVA. Black data point represents mean value of each group. *D*: ordinary least squares regression analysis (OLS) of mean $\log_2$ fold change (FC) in ASR [stimulated (Stim)/control (Ctrl)] across the early (0–10 days) period of PRT and the quantified $\log_2$ FC in abundance (Stim/Ctrl) on *day 10* ($n = 216$ proteins). *E* and *F*: multiple regression analysis of changes in predicted protein abundance ($\log_2$ Stim/Ctrl) after 20 (*E*) and 30 (*F*) days of PRT calculated from ASRs quantified across the preceding measurement periods. Quantified FC ($\log_2$ Stim/Ctrl) in protein-specific ASR across early and mid (*E*) and early, mid, and late (*F*) experimental periods were used to predict *day 20* and *day 30* protein abundances, respectively. Data reported from $n = 4$ biological replicates per time point (0, 10, 20, and 30 days) and condition (Stim and Ctrl).

protein abundance; however, the low slope (0.274) of the linear regression shows that only a small proportion of the protein synthesized was ultimately accreted into muscle protein. Multiple linear regression on changes in ASR across both the early and mid experimental periods (Fig. 5*E*) explained ~65% of the gain in muscle protein content after 20 days of resistance training. The elevation in ASR across early, mid, and late experimental periods explained ~50% of the gain in protein content after 30 days of training (Fig. 5*F*).

An imbalance between changes in protein synthesis and accretion (termed "oversynthesis") was also evident at the protein-specific level. For example, during the first 10 days of resistance training, ribosomal protein S6 (RS6) accumulated at a rate of 65.77 ± 33.16 ng/day in stimulated muscle compared to 0.933 ± 9.47 ng/day in control muscle. The increase in RS6 protein abundance in stimulated muscle was underpinned by a 7.4-fold increase in ASR (stimulated: 162.61 ± 101.01 ng/day vs. control: 21.96 ± 12.00 ng/day) and a 4.6-fold increase in absolute degradation rate (stimulated: 96.83 ± 69.49 ng/day vs. control: 46.78 ± 8.69 ng/day). Therefore, both the abundance and turnover rate of RS6 were increased in exercised muscle (Fig. 6, *A–C*) and only ~40% of RS6 protein synthesized in stimulated muscle was retained and contributed to the gain in abundance of new muscle protein.

The ASR of ATP synthase subunit-β (ATPB; included in ABD_Cluster_2) was 3.6-fold greater ($P = 0.037$) specifically during the mid (10–20 days) experimental period. In control muscle, between *day 10* and *day 20* the ASR of ATPB was 8.40 ± 4.90 µg/day and the rate of change in ATPB abundance was 3.15 ± 7.76 µg/day, which gives a calculated degradation rate for ATPB of 5.25 ± 2.91 µg/day in nonexercised muscle. In stimulated muscle, during the same 10–20 days the ASR of ATPB was 30.39 ± 18.67 µg/day (~3.6-fold greater than control), ATPB abundance increased at a rate of 17.35 ± 12.36 µg/day, and the calculated degradation rate was 13.04 ± 6.97 µg/day (~2.5-fold greater than control) (Fig. 6, *D–F*). Therefore, in exercised muscle only ~38% of newly synthesized ATPB was retained and contributed to the gain in new muscle protein.

Unsupervised clustering and network analyses of changes in individual protein ASR (Fig. 7, *A–C*) highlighted

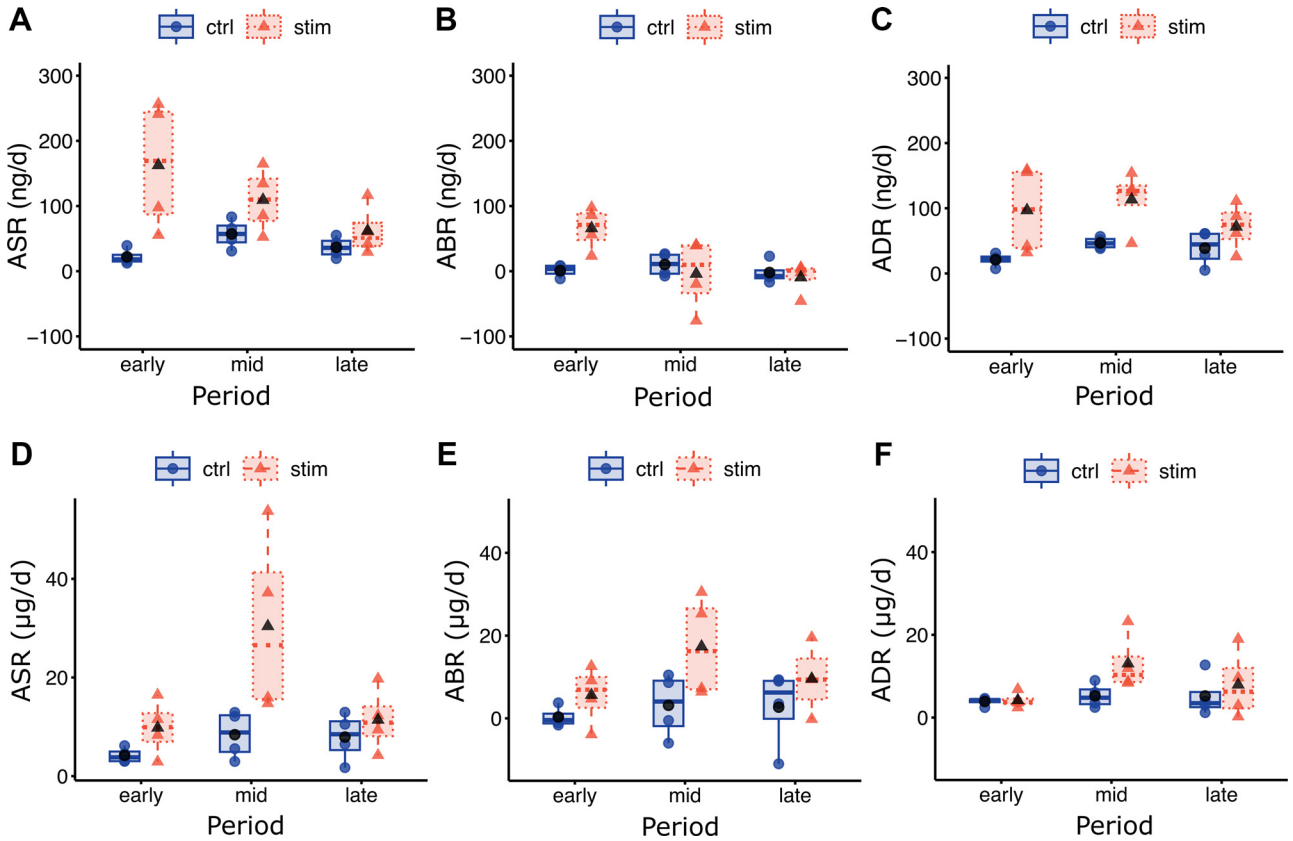

Figure 6. Absolute Dynamic Profiling Technique for Proteomics (Proteo-ADPT) analysis of programmed resistance training (PRT)-induced muscle growth. Application of the Proteo-ADPT used to explain how changes in protein accumulation (abundance rate of change) occur during adaptation to PRT. Boxplots of Proteo-ADPT data quantified across the entire experimental design for ribosomal protein S6 (RS6; *A*–*C*) and ATP synthase subunit beta (ATPB; *D*–*F*), including absolute protein synthesis rate (ASR; *A* and *D*), abundance rate of change (ABR; *B* and *E*), and subsequent calculation of absolute protein degradation rate (ADR; *C* and *F*), highlighting that the rate of protein synthesis of ATPB was greater (*D*) than degradation (*F*) during the mid period of adaptation, resulting in protein accumulation (*E*), whereas for RS6 protein synthesis (*A*) and degradation (*C*) were equal, resulting in no further accumulation of ribosomal protein across mid or later adaptation (*B*). Black data points represent mean value of each condition. Data reported from $n = 4$ biological replicates per time point (0, 10, 20, and 30 days) and condition [stimulated (Stim) and control (Ctrl)].

three patterns of response. ASR_Cluster_1 comprised 44 proteins that were upregulated in ASR specifically during the early (0–10 days) response to programmed resistance training, including proteins involved in translation (6 ribosomal proteins: RS-SA, -6, -9, -19, -20, and RL6 and eEF1G, eF2, and EFTU). ASR_Cluster_1 also included proteins associated with muscle growth and development (MYH3, MYH8, CRYAB, TRDN and DESM; Fig. 7*A*) and glycolytic enzymes (ALDOA, ENOB, ODPA, ODP2, PHKG2, PYGM, PGM1 and PFKM).

Proteins in ASR_Cluster_2 (54 proteins) exhibited greater ASR during both early and mid experimental periods compared to the late (20–30 days) experimental period and contained two subnetworks of proteins associated with muscle contraction (12 proteins including: DMD, TPM1, TNNT3, MYH7, ACTS1, MYL1, MYBPC1, AT2A1, JPH2, RYR1, KLH41 and CACB1) and a network of 24 proteins annotated to the GO cellular compartment "mitochondrion" (Fig. 7*B*). Proteins in ASR_Cluster_3 (19 proteins) exhibited greater ASR in exercised muscle specifically during the mid period, and the majority (17/19 proteins) were associated with metabolic process, including 13 proteins annotated to the mitochondria (Fig. 7).

DISCUSSION

We have used Proteo-ADPT, which builds on recent developments in deuterium oxide labeling and peptide mass spectrometry to simultaneously investigate the abundance and synthesis of individual proteins in absolute (grams) rather than relative (%) terms. Traditional proteomic techniques that report the relative abundance profile of proteins are insufficient for studying interventions, such as resistance exercise training, in which significant changes in muscle mass are expected. Similarly, isotope labeling studies that measure only fractional (relative; %/day) synthesis rates (FSRs) cannot distinguish between *1*) changes in protein synthesis that lead to gains in protein abundance and *2*) increases to the turnover rate of proteins that are not accompanied by changes in protein content. Proteo-ADPT reports absolute data on both the abundance and synthesis rate of individual proteins and, in the present work, generated new insight into muscle responses to resistance exercise training. Our findings highlight that young healthy male rats have more than ample capacity to synthesize new protein, which suggests that further improvements in muscle growth responses to

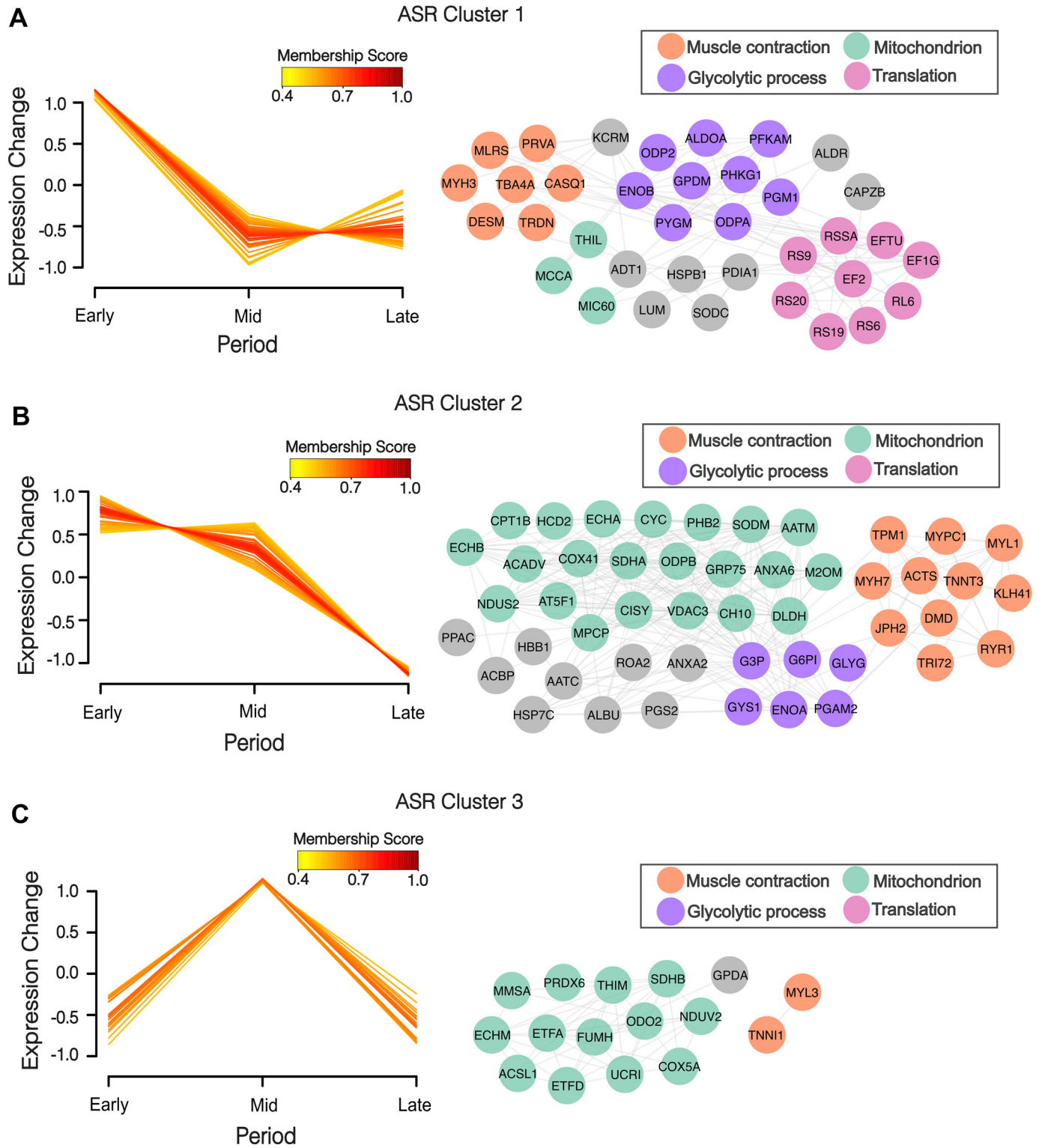

Figure 7. Time course changes in synthesis rates occurring during programmed resistance training (PRT)-induced muscle growth. *A–C*: temporal profiles [$\log_2$ transformed stimulated (Stim)/control (Ctrl)l fold difference at each time point] of individual protein absolute synthesis rates (ASRs) ($n = 216$ proteins) underwent soft clustering analysis using the fuzzy *c*-means clustering algorithm with the Mfuzz R package to assess temporal profiles of changes in ASR ($\log_2$ Stim/Ctrl) across early, mid, and later adaptation to PRT. The minimum membership value for inclusion into a cluster was set at 0.5. Search Tool for the Retrieval of INteracting Genes/proteins (STRING) protein interaction network for proteins contained in Cluster 1 (*A*) (increased in synthesis rate early in adaptation), Cluster 2 (*B*) (increased in synthesis across early and mid adaptive periods), and Cluster 3 (*C*) (specifically increased in ASR during mid adaptive period of PRT) reported. Node color represents subnetworks of proteins manually annotated to different functional groups comprising temporal profiles including ribosome/translation (purple), muscle contraction and organization (orange), mitochondria (green), and glycolytic enzymes (blue). Data reported from $n = 4$ biological replicates per time point (0, 10, 20, and 30 days) and condition (Stim and Ctrl).

exercise could be made by attempting to manipulate the "conversion factor," i.e., the ratio between protein synthesis and protein accretion, rather than focusing solely on maximizing protein synthetic responses. Furthermore, we discovered different temporal patterns of adaptation among subsets of muscle proteins, highlighting that protein accretion during resistance training does not occur in a uniform manner. Rather, subsets of proteins can accumulate in muscle at different rates across a period of adaptation, such as early ribosomal accretion followed by later mitochondrial accumulation. These novel insights into the temporal patterns of muscle protein accretion are summarized in the graphical abstract and add useful context to existing literature based on static data from measurements at isolated time points. For example, our findings help consolidate long-standing questions surrounding the nature and timing of mitochondrial adaptation during hypertrophy by revealing that mitochondrial expansion occurs, but later and more slowly than ribosomal and contractile protein accretion.

In humans, it is recognized that the acute increases in mixed-protein FSR that occur after the initial bouts of resistance exercise do not predict the magnitude of subsequent muscle growth after longer-term resistance training (27). Similarly, in rats markers of the activation of translation initiation, such as p70s6K phosphorylation, exhibit relatively large acute increases to contractile stimuli compared to the subsequent gains in muscle growth (28). Our data (Fig. 5*D*) demonstrate that a relatively small (on average ~27%) proportion of newly synthesized protein is retained and contributes to gains in muscle protein content in response to resistance training. This relatively small "conversion factor" between synthesis and accretion is evidence that protein degradative processes are also prominently activated by exercise. Transcriptomic profiling in this model of resistance training (15) shows that genes associated with phagosomal and lysosomal processes are more highly expressed throughout the 30-day period of adaptation. These findings in rat align with the heightened activation of chaperone-assisted selective autophagy in human muscle during the initial adaptation to resistance exercise training (29).

The present Proteo-ADPT analysis provides empirical data that the turnover of protein is increased, in addition to protein accretion, in muscle exposed to a resistance training stimulus. We interpret the heightened turnover of muscle protein as a positive and necessary mechanism of muscle adaptation to exercise training. That is, higher levels of protein turnover are necessary to replace proteins damaged by the additional mechanical and metabolic load of heavy exercise and, therefore, help to maintain or improve muscle protein homeostasis (11). Our findings raise the question of whether gains in muscle mass in response to resistance training could be further optimized by exploring interventions that increase the conversion of newly synthesized protein into the accretion of muscle protein content or whether the pursuit of enhancing the conversion of newly synthesized protein into muscle protein accretion could diminish muscle protein quality and negatively impact muscle function. In the future, it will be exciting to use Proteo-ADPT to investigate whether disease- or age-related losses in muscle mass are associated with changes to the conversion factor between the synthesis and accretion of muscle protein.

Increases in the relative abundance of ribosomal proteins have been reported in humans after 4 wk (3 times per week) of resistance training (RT) (30), but other work reported no changes in ribosomal content after a longer-term, 8-wk, RT intervention (31). Our time series analysis of absolute abundance data adds context regarding the sequential process of adaptation and helps the interpretation of the aforementioned relative abundance measurements in humans. r-Protein abundance is tightly controlled, and gains in r-proteins plateaued after *day 10* and remained stable across the final 20 days of resistance training (Fig. 3), during which there was little further increase in muscle weight despite ongoing daily training. Excess ribosomal subunits may be rapidly degraded by the ubiquitin proteasome system (32), but our protein-specific analysis of RS6 (Fig. 6) shows that the plateau in ribosomal protein abundance was brought about by changes to both the synthesis and degradation rate. That is, compared to the early adaptive period, the ASR of RS6 protein fell by 33% in Stim TA and the ADR of RS6 increased by 17% in the mid (10–20 days) experimental period, and both the ASR and ADR of RS6 further declined during the late (20–30 days) period.

Mechanical loading by resistance training enhances the expression of genes encoding ribosomal proteins (15) and is associated with greater expression of ribosomal RNA (rRNA) (33), indicating that gains in ribosomal biogenesis are associated with increases in muscle mass. Synergist ablation has been a key experimental model for studying muscle hypertrophy and protein accretion in rats and is associated with increases in translational capacity based on the increase in rRNA (34) and total RNA content (35) of hypertrophied muscle. Translational capacity in terms of grams of protein synthesized and relative to the content of ribosomal protein (r-protein) have been less studied but are important because ribosomal proteins are integral components of the ribosome and are involved in the process of muscle growth. Ribosomal proteins have essential roles in rRNA processing, including ribosome maturation, assembly, stability, and translational fidelity (36), and are known to be less abundant in the muscle of older adults (37). In the present work, time series analysis highlighted the coregulation of 18 r-proteins (8 small and 10 large subunit proteins) that significantly increased during the first 10 days of muscle growth in response to programmed resistance training. Similarly, the total protein content of all 40S (sum of 26 proteins) and 60S (sum of 30 proteins) ribosomal subunits measured in this work exhibited comparable patterns of response, and there was a consistent ratio between r-protein content and the total amount of protein synthesized (i.e., absolute synthesis per μg of r-protein), which remained stable at ~30 μg of protein synthesized per microgram of r-protein per day throughout the period of muscle growth. Our findings support the key role of ribosomal biogenesis in the response of muscle to resistance exercise, and future exploitation of Proteo-ADPT and programmed resistance training could show whether the abbreviated molecular responses to acute exercise in the muscle of older rats (38) equate to blunted muscle protein

accretion and/or a lesser uplift in protein turnover and proteome quality.

Mitochondrial adaptations are universally accepted in response to endurance exercise, whereas the impact of resistance training on mitochondrial biogenesis and content is still debated (39). Early electron microscopy studies suggested that mitochondrial volume may be diluted by gains in muscle mass associated with resistance training (40, 41), whereas data on the relative abundance of mitochondrial proteins, such as citrate synthase, suggest there are no changes in mitochondrial volume in resistance-trained muscle (42). Gains in muscle mass induced by the ablation (35) or tenotomy (43) of synergist muscles are associated with elevations in the fractional synthesis rate of protein mixtures from both the myofibrillar and soluble fractions of rat muscle, which would be expected to each include mitochondrial proteins. Our protein-specific analysis highlights that mitochondrial adaptation is a prominent component of the muscle response to daily programmed resistance training but occurs after the initial increase in ribosomal protein content. Total mitochondrial protein content increased in line with protein-specific responses in Abundance Cluster 2 (Fig. 4*C*), which suggests reasonably coordinated gains in mitochondrial protein, but, interestingly, two mitochondrially encoded proteins, NADH-ubiquinone oxidoreductase chains -1 and -4 (NU1M and NU4M), were in ABD_cluster_1 and increased in abundance before the gains in abundance of the other detected mitochondrial proteins. These findings suggest that although mitochondrial protein accretion is a core feature of adaptation following 10–20 days of programmed resistance training, mitochondrial remodeling during resistance training may not be a uniform process. Rather, selective changes in mitochondrially encoded proteins may occur before more coordinated, bulk increases in mitochondrial content are established.

Although mitochondrial adaptation was evident in our proteomic data, transcriptomic responses reported previously (15) did not follow the same temporal pattern. For example, during the intermediate (10–20 days) period, ATP synthase subunits alpha (ATPA) and beta (ATPB) exhibited a greater than twofold increase in synthesis in response to programmed resistance training, whereas, in our transcriptomic analysis of this model, increases in mRNA expression of mitochondria- and oxidative phosphorylation-related proteins only occurred after 20–30 days of programmed resistance training (15). These findings are similar to the disconnection between changes in mRNA expression and protein abundance, particularly for mitochondrial proteins reported in human muscle responses to exercise training (44). Most mitochondrial proteins are nuclear encoded, translated on cytosolic ribosomes, and imported into mitochondria via the translocases of the outer and inner membranes before processing and assembly. Consequently, a simple mRNA:protein relationship is not expected (45). In human skeletal muscle, endurance training increases mitochondrial protein abundance without proportionate changes in the transcription of corresponding mRNAs (46). The discordance between nuclear-encoded mitochondrial gene expression and protein content may be due to additional levels of regulation, e.g., during translocation, in addition to differences in the time lag between mRNA transcription and protein accrual for mitochondrial proteins. Future studies are required to directly quantify how exercise alters the import, assembly, and selective degradation of mitochondrial proteins and identify the specific posttranscriptional checkpoints that drive changes in mitochondrial protein content and function despite potentially no corresponding changes in gene expression.

It is well established that unaccustomed exercise or contraction-induced loading of muscle is associated with transient disruptions in myofibril structure, which can be evidenced by z-band streaming (47). Although we saw no fiber damage in histological sections, during the early period of adaption to resistance training (Fig. 3*A*) proteins associated with myofibril proteostasis, including α-crystallin B chain (CRYAB), heat shock protein beta-2 (HSPB2), and vimentin, increased in abundance. In addition, desmin and embryonic myosin heavy chain (MYH3) exhibited higher rates of synthesis only during the early adaptation period (Fig. 7*A*). It is important, however, to delineate the difference between evidence of damage/disorganization at the myofibril level from processes of muscle fiber necrosis and degeneration, which are not seen in this model of resistance exercise training (48, 49).

Small heat shock proteins, including HSPB2 and CRYAB, act as molecular chaperones to prevent protein aggregation and promote refolding or degradation of damaged proteins (50). CRYAB is a well-known exercise-responsive heat shock protein in muscle that protects against unfolding and aggregation of myosin heavy chains (51) and translocates to myofibril z disks and desmin structures after damaging eccentric contractions (52). Phosphorylation of CRYAB S59 co-occurs with the translocation of CRYAB to cytoskeletal structures after unaccustomed exercise, and the magnitude of this response subsides with subsequent exercise bouts alongside gradual increases in the abundance of the intermediate filament protein desmin (53). In humans, phosphorylation of CRYAB S59 is part of the sustained signaling response that is specific to resistance exercise (54), and the turnover rates of CRYAB and desmin increase during a 9-day period of resistance exercise training (8). Collectively, these findings and our present data point to key roles of CRYAB and desmin in the remodeling of myofibril structure as part of the early adaptive process of muscle to resistance exercise.

Increases in the abundance of vimentin and the synthesis rate of MYH3 may indicate activation of the myogenic program during the early adaptation to resistance training. Vimentin is an interfilament protein, similar to desmin, but vimentin is expressed early during muscle regeneration, whereas desmin is more prominent in adult muscle fibers (55). Muscle growth after 10 days of synergist ablation in mice is associated with a significant increase in vimentin that is primarily localized to muscle satellite cells (52), and, traditionally, detection of MYH3 in adult muscle is considered a marker of muscle regeneration (56). In our histological studies on this model of muscle growth, we have not detected small fibers with centralized nuclei, which evidence fiber regeneration (48). It is possible, however, that our more detailed proteomic analyses show that disruption at the myofibril level, e.g., desmin and CRYAB responses discussed above, is sufficient to instigate a level of activation of the

myogeneic program that is not accompanied by traditional markers of fiber regeneration. Indeed, MYH3-positive fibers are not detected in healthy adult muscle by immunohistochemical methods (56), yet small amounts of MYH3 are detectable by mass spectrometry in adult muscles of rodents (57) and humans (58) under normal habitual conditions. In the present work, MYH3 abundance was an order of magnitude less than adult fast-twitch type IIb (87 ± 28 ng compared to 28.5 ± 3.5 µg; see Supplemental Material), and programmed resistance exercise did not increase MHY3 abundance but did increase the turnover rate of MYH3 specifically during the early adaptation period. Therefore, our findings add to growing data on the activation of classical damage response pathways without the requirement for gross fiber damage.

Activation of the myogenic program is detectable during the early response to resistance exercise in humans, and pathways exist for the activation of satellite cells, such as HeyL (59), that are not essential to regeneration after degenerative damage but are required for growth of overloaded muscle. In addition to its connection with satellite cells (52), vimentin is implicated in the regulation of cell size (60), and in muscle the increase in vimentin abundance could be a core component of the adaptive response to contractile work rather than a secondary response to damaging exercise. Chen et al. (61) demonstrated that translational control mechanisms target specific mRNAs, including HSPB2, to the actively translating polysome fraction after unaccustomed high-resistance contractions. Translational control is associated with transcripts containing 5′ terminal oligopyrimidine (5′ TOP) tracts (62), and vimentin mRNA contains a 5′ TOP motif (63). Other proteins encoded by mRNAs with 5′ TOP motifs, such as ribosomal proteins (RS-SA, -6, -9, -19, -20, and RL6) and elongation factors (eF1G and eEF2), also exhibited early gains in protein abundance (Fig. 3) and greater rates of synthesis (Fig. 7) primarily during the first 10 days of exercise-induced growth. In skeletal muscle, these responses may be driven by Myc, which is a central component of the acute immediate early gene transcriptional response to the initial bouts of resistance exercise and later subsides after longer periods of training (15, 64, 65).

Future studies incorporating single-cell analyses or proximity labeling techniques with Proteo-ADPT could uncover further detail regarding the activation of the myogenic program in response to resistance exercise training. Here, we used differential centrifugation to separate myofibrillar (pellet) and soluble (supernatant) proteins to improve the analytical depth of our proteomic analysis rather than to infer subcellular localization. Compared to other tissues, striated muscle is a challenging substrate for proteomic analysis (66), and sample fractionation enables a greater total number of proteins to be studied despite the prevalence of a small number of highly abundant myofibrillar proteins. To preserve the integrity of our absolute quantification, data from the pellet and supernatant fractions were reintegrated into single protein-level values, which prevents compartment-specific interpretation such as translocation of CRYAB from soluble to myofibrillar fraction. We also did not investigate fiber type-specific adaptations, but prior work using an identical program of resistance training (15) demonstrated comparable hypertrophy across type I, IIA, and IIX fibers that may be attributed to the uniform motor unit recruitment occurring during nerve stimulation. That said, this model of daily training decreases the mRNA expression of fast-twitch myosin heavy chain isoforms (15), and here we report that daily resistance training specifically increased synthesis of the adult type I myosin heavy chain (MYH7) during the early and mid periods of adaptation (ASR_Cluster_2; Fig. 7*B*).

The mitochondrial protein response may be particular to our model of daily resistance training, which uses electrical stimulation to evoke primarily maximal isometric contractions of the tibialis anterior, producing uniform motor unit recruitment and high force during each repetition without variation in effort or load. Future studies using less frequent training, e.g., 3 days per week similar to recreational training practices in humans, may exhibit less prominent mitochondrial adaptation, but differences in muscle fiber type may also need to be considered. The tibialis anterior of rat is a predominantly fast-twitch muscle, whereas human resistance training interventions primarily study the vastus lateralis, which consists of a mixture of fast- and slow-twitch fibers. Notwithstanding the differences between electrical stimulation and voluntary human resistance training in contraction mode, frequency, and muscle fiber type, our model in vivo provides a physiologically relevant anabolic stimulus with high experimental control. Our rat study helps to clarify long-standing questions about the timing of mitochondrial adaptation during hypertrophy, showing that mitochondrial expansion does occur but follows ribosomal and contractile protein accretion. Recognizing these distinct phases of adaptation may reconcile conflicting findings in the literature and guide the design of future human studies. For instance, training interventions could be structured to prioritize early ribosomal and myofibrillar growth before progressing to higher-volume or endurance-oriented elements that support mitochondrial development, thereby aligning the training stimulus with the sequential molecular processes underpinning resistance training adaptation.

The present study did not include female rats, and sexual dimorphism in the dynamic proteome response of muscle to exercise cannot be ruled out. In humans, Scalzo et al. (67) report greater mitochondrial protein synthesis in males compared to females during sprint interval training, and Smith et al. (68) report higher basal levels of muscle protein synthesis but lesser exercise-induced gains in protein synthesis in obese older women compared to age-matched obese men. Rat muscle responses to hindlimb unloading may also differ in a sex-specific manner. In male rats, the loss of muscle cross-sectional area in response to unloading is associated with a decrease in mixed-myofibrillar protein synthesis rates (69), whereas equivalent work in females (70) found that an increase in protein degradation was associated with the loss in muscle cross sectional area. Our unpublished preliminary analyses also suggest that differences in protein-specific turnover rates may exist between male and female rats under control conditions. Analysis (Burniston, Stead, Jarvis, unpublished observations) of 309 proteins in tibialis anterior collected from male and female rats after 0, 5, 10, 15, and 20 days of deuterium oxide consumption ($n = 1$ male and $n = 1$

female at each time point) found that 52 proteins had >2 SD difference in turnover rate between males and females, including iron metabolism proteins that had higher turnover in females and enzymes of fatty acid β-oxidation that had higher turnover in males. Some ribosomal subunits (40S ribosomal protein SA and 40S ribosomal protein S3) exhibited differences in turnover rate between male and female rats under control conditions; therefore, we cannot exclude the possibility that the protein-specific changes in synthesis and degradation reported here in males may not be conserved in the adaptive response to programmed resistance training in females. The door is open for future exciting studies on sexual dimorphism and age-related differences in dynamic proteome responses to exercise training.

Conclusions

Programmed resistance training led to significant increases in muscle protein content, reflecting muscle growth. Our Absolute Dynamic Profiling Technique for Proteomics (Proteo-ADPT) revealed that this growth was underpinned by time-dependent changes in both protein synthesis and accumulation. During the early period of adaptation, the increase in protein synthesis rates was not matched by equivalent gains in protein abundance, suggesting concomitant increases in protein degradation that enhance protein turnover. Furthermore, we identified that distinct proteome components (e.g., ribosomal vs. mitochondrial proteins) exhibited different timelines of expansion. These findings highlight how dynamic, time-resolved, and absolute quantification can uncover regulatory features of muscle adaptation that are not evident from static or relative measurements alone. Rather than a uniform hypertrophic program, muscle growth appears to involve temporally structured remodeling. This has important implications for training design: it suggests that the timing and sequencing of stimuli, for instance, prioritizing ribosomal and myofibrillar adaptations early followed by later metabolic support, may be a critical but underappreciated variable in exercise prescription. Further development and application of Proteo-ADPT may help guide such strategies, enabling interventions that optimize not just protein synthesis but the effective conversion of synthesis into retained muscle protein mass.

ETHICS APPROVAL

Experimental procedures were conducted under the auspices of the British Home Office Animals (Scientific Procedures) Act 1986 (License number: PA693D221).

DATA AVAILABILITY

The mass spectrometry proteomics data have been deposited to the ProteomeXchange Consortium via the PRIDE partner repository with the dataset identifiers PXD060879 and 10.6019/PXD060879.

SUPPLEMENTAL MATERIAL

Supplemental Tables S1 and S2: https://doi.org/10.6084/m9.figshare.30103390.

ACKNOWLEDGMENTS

Present addresses: S. J. Hesketh: University of Central Lancashire, School of Medicine, Preston, PR1 2HE, United Kingdom; M. R. Viggars: Dept. of Physiology and Aging, University of Florida, Gainesville, FL, United States.

DISCLOSURES

No conflicts of interest, financial or otherwise, are declared by the authors.

AUTHOR CONTRIBUTIONS

J.C.J. and J.G.B. conceived and designed research; C.A.S., S.J.H., A.C.Q.T., M.R.V., H.S., J.C.J., and J.G.B. performed experiments; C.A.S., S.J.H., A.C.Q.T., and J.G.B. analyzed data; C.A.S., S.J.H., A.C.Q.T., and J.G.B. interpreted results of experiments; C.A.S. prepared figures; C.A.S., S.J.H., A.C.Q.T., M.R.V., H.S., J.C.J., and J.G.B. drafted manuscript; C.A.S., S.J.H., A.C.Q.T., M.R.V., H.S., J.C.J., and J.G.B. edited and revised manuscript; C.A.S., S.J.H., A.C.Q.T., M.R.V., H.S., J.C.J., and J.G.B. approved final version of manuscript.

REFERENCES

1. **Mcleod JC**, **Stokes T**, **Phillips SM.** Resistance exercise training as a primary countermeasure to age-related chronic disease. *Front Physiol* 10: 645, 2019. doi:10.3389/fphys.2019.00645.
2. **Hesketh SJ**, **Stansfield BN**, **Stead CA**, **Burniston JG.** The application of proteomics in muscle exercise physiology. *Expert Rev Proteomics* 17: 813–825, 2020. doi:10.1080/14789450.2020.1879647.
3. **Roberts MD**, **McCarthy JJ**, **Hornberger TA**, **Phillips SM**, **Mackey AL**, **Nader GA**, **Boppart MD**, **Kavazis AN**, **Reidy PT**, **Ogasawara R**, **Libardi CA**, **Ugrinowitsch C**, **Booth FW**, **Esser KA.** Mechanisms of mechanical overload-induced skeletal muscle hypertrophy: current understanding and future directions. *Physiol Rev* 103: 2679–2757, 2023. doi:10.1152/physrev.00039.2022.
4. **Davies RW**, **Lynch AE**, **Kumar U**, **Jakeman PM.** Characterisation of the muscle protein synthetic response to resistance exercise in healthy adults: a systematic review and exploratory meta-analysis. *Transl Sports Med* 2024: 3184356, 2024. doi:10.1155/2024/3184356.
5. **Phillips SM**, **Tipton KD**, **Aarsland A**, **Wolf SE**, **Wolfe RR.** Mixed muscle protein synthesis and breakdown after resistance exercise in humans. *Am J Physiol Endocrinol Metab* 273: E99–E107, 1997. doi:10.1152/ajpendo.1997.273.1.E99.
6. **Brook MS**, **Wilkinson DJ**, **Mitchell WK**, **Lund JN**, **Szewczyk NJ**, **Greenhaff PL**, **Smith K**, **Atherton PJ.** Skeletal muscle hypertrophy adaptations predominate in the early stages of resistance exercise training, matching deuterium oxide-derived measures of muscle protein synthesis and mechanistic target of rapamycin complex 1 signaling. *FASEB J* 29: 4485–4496, 2015. doi:10.1096/fj.15-273755.
7. **Burniston JG.** Investigating muscle protein turnover on a protein-by-protein basis using dynamic proteome profiling. In: *Omics Approaches to Understanding Muscle Biology*, edited by Burniston JG, Chen YW**.** Springer US, 2019, p. 171–190.
8. **Camera DM**, **Burniston JG**, **Pogson MA**, **Smiles WJ**, **Hawley JA.** Dynamic proteome profiling of individual proteins in human skeletal muscle after a high-fat diet and resistance exercise. *FASEB J* 31: 5478–5494, 2017. doi:10.1096/fj.201700531R.
9. **Murphy CH**, **Shankaran M**, **Churchward-Venne TA**, **Mitchell CJ**, **Kolar NM**, **Burke LM**, **Hawley JA**, **Kassis A**, **Karagounis LG**, **Li K**, **King C**, **Hellerstein M**, **Phillips SM.** Effect of resistance training and protein intake pattern on myofibrillar protein synthesis and proteome kinetics in older men in energy restriction. *J Physiol* 596: 2091–2120, 2018. doi:10.1113/JP275246.
10. **Shankaran M**, **Shearer TW**, **Stimpson SA**, **Turner SM**, **King C**, **Wong PY**, **Shen Y**, **Turnbull PS**, **Kramer F**, **Clifton L**, **Russell A**, **Hellerstein MK**, **Evans WJ.** Proteome-wide muscle protein fractional synthesis rates predict muscle mass gain in response to a selective

androgen receptor modulator in rats. *Am J Physiol Endocrinol Metab* 310: E405–E417, 2016. doi:10.1152/ajpendo.00257.2015.
11. **Srisawat K**, **Stead CA**, **Hesketh K**, **Pogson M**, **Strauss JA**, **Cocks M**, **Siekmann I**, **Phillips SM**, **Lisboa PJ**, **Shepherd S**, **Burniston JG.** People with obesity exhibit losses in muscle proteostasis that are partly improved by exercise training. *Proteomics* 24: e2300395, 2024. doi:10.1002/pmic.202300395.
12. **Hesketh SJ**, **Sutherland H**, **Lisboa PJ**, **Jarvis JC**, **Burniston JG.** Adaptation of rat fast-twitch muscle to endurance activity is underpinned by changes to protein degradation as well as protein synthesis. *FASEB J* 34: 10398–10417, 2020. doi:10.1096/fj.202000668RR.
13. **Brown AD**, **Stewart CE**, **Burniston JG.** Degradation of ribosome and chaperone proteins is attenuated during the differentiation of replicatively aged C2C12 myoblasts. *J Cachexia Sarcopenia Muscle* 13: 2562–2575, 2022. doi:10.1002/jcsm.13034.
14. **Schmoll M**, **Unger E**, **Sutherland H**, **Haller M**, **Bijak M**, **Lanmüller H**, **Jarvis JC.** Spillover stimulation: a novel hypertrophy model using co-contraction of the plantar-flexors to load the tibial anterior muscle in rats. *PLoS One* 13: e0207886, 2018. doi:10.1371/journal.pone.0207886.
15. **Viggars MR**, **Sutherland H**, **Lanmüller H**, **Schmoll M**, **Bijak M**, **Jarvis JC.** Adaptation of the transcriptional response to resistance exercise over 4 weeks of daily training. *FASEB J* 37: e22686, 2023. doi:10.1096/fj.202201418R.
16. **Wiśniewski JR**, **Zougman A**, **Nagaraj N**, **Mann M.** Universal sample preparation method for proteome analysis. *Nat Methods* 6: 359–362, 2009. doi:10.1038/nmeth.1322.
17. **Silva JC**, **Gorenstein MV**, **Li GZ**, **Vissers JP**, **Geromanos SJ.** Absolute quantification of proteins by LCMSE. *Mol Cell Proteomics* 5: 144–156, 2006. doi:10.1074/mcp.M500230-MCP200.
18. **McCabe BJ**, **Bederman IR**, **Croniger C**, **Millward C**, **Norment C**, **Previs SF.** Reproducibility of gas chromatography–mass spectrometry measurements of ^{2}H labeling of water: application for measuring body composition in mice. *Anal Biochem* 350: 171–176, 2006. doi:10.1016/j.ab.2006.01.020.
19. **Nishimura Y**, **Bittel AJ**, **Stead CA**, **Chen YW**, **Burniston JG.** Facioscapulohumeral muscular dystrophy is associated with altered myoblast proteome dynamics. *Mol Cell Proteomics* 22: 100605, 2023. doi:10.1016/j.mcpro.2023.100605.
20. **Sadygov RG.** Partial isotope profiles are sufficient for protein turnover analysis using closed-form equations of mass isotopomer dynamics. *Anal Chem* 92: 14747–14753, 2020. doi:10.1021/acs.analchem.0c03343.
21. **Holmes WE**, **Angel TE**, **Li KW**, **Hellerstein MK.** Dynamic proteomics: in vivo proteome-wide measurement of protein kinetics using metabolic labeling. *Methods Enzymol* 561: 219–276, 2015. doi:10.1016/bs.mie.2015.05.018.
22. **Ilchenko S**, **Haddad A**, **Sadana P**, **Recchia FA**, **Sadygov RG**, **Kasumov T.** Calculation of the protein turnover rate using the number of incorporated ^{2}H atoms and proteomics analysis of a single labeled sample. *Anal Chem* 91: 14340–14351, 2019. doi:10.1021/acs.analchem.9b02757.
23. **Storey JD**, **Tibshirani R.** Statistical significance for genomewide studies. *Proc Natl Acad Sci USA* 100: 9440–9445, 2003. doi:10.1073/pnas.1530509100.
24. **Kumar L**, **Futschik M.** Mfuzz: a software package for soft clustering of microarray data. *Bioinformation* 2: 5–7, 2007. doi:10.6026/97320630002005.
25. **Szklarczyk D**, **Gable AL**, **Lyon D**, **Junge A**, **Wyder S**, **Huerta-Cepas J**, **Simonovic M**, **Doncheva NT**, **Morris JH**, **Bork P**, **Jensen LJ**, **Von Mering C.** STRING v11: protein-protein association networks with increased coverage, supporting functional discovery in genome-wide experimental datasets. *Nucleic Acids Res* 47: D607–D613, 2019. doi:10.1093/nar/gky1131.
26. **Shannon P**, **Markiel A**, **Ozier O**, **Baliga NS**, **Wang JT**, **Ramage D**, **Amin N**, **Schwikowski B**, **Ideker T.** Cytoscape: a software environment for integrated models of biomolecular interaction networks. *Genome Res* 13: 2498–2504, 2003. doi:10.1101/gr.1239303.
27. **Mitchell CJ**, **Churchward-Venne TA**, **Parise G**, **Bellamy L**, **Baker SK**, **Smith K**, **Atherton PJ**, **Phillips SM.** Acute post-exercise myofibrillar protein synthesis is not correlated with resistance training-induced muscle hypertrophy in young men. *PLoS One* 9: e89431, 2014 [Erratum in *PLoS One* 9: e98731, 2014]. doi:10.1371/journal.pone.0089431.
28. **Baar K**, **Esser K.** Phosphorylation of p70S6k correlates with increased skeletal muscle mass following resistance exercise. *Am J Physiol Cell Physiol* 276: C120–C127, 1999. doi:10.1152/ajpcell.1999.276.1.C120.
29. **Ulbricht A**, **Gehlert S**, **Leciejewski B**, **Schiffer T**, **Bloch W**, **Höhfeld J.** Induction and adaptation of chaperone-assisted selective autophagy CASA in response to resistance exercise in human skeletal muscle. *Autophagy* 11: 538–546, 2015. doi:10.1080/15548627.2015.1017186.
30. **Jessen S**, **Quesada JP**, **Di Credico A**, **Moreno-Justicia R**, **Wilson R**, **Jacobson G**, **Bangsbo J**, **Deshmukh AS**, **Hostrup M.** Beta2-adrenergic stimulation induces resistance training-like adaptations in human skeletal muscle: potential role of KLHL41. *Scand J Med Sci Sports* 34: e14736, 2024. doi:10.1111/sms.14736.
31. **Roberts MD**, **Ruple BA**, **Godwin JS**, **McIntosh MC**, **Chen SY**, **Kontos NJ**, **Agyin-Birikorang A**, **Michel M**, **Plotkin DL**, **Mattingly ML**, **Mobley B**, **Ziegenfuss TN**, **Fruge AD**, **Kavazis AN.** A novel deep proteomic approach in human skeletal muscle unveils distinct molecular signatures affected by aging and resistance training. *Aging (Albany NY)* 16: 6631–6651, 2024. doi:10.18632/aging.205751.
32. **Lam YW**, **Lamond AI**, **Mann M**, **Andersen JS.** Analysis of nucleolar protein dynamics reveals the nuclear degradation of ribosomal proteins. *Curr Biol* 17: 749–760, 2007. doi:10.1016/j.cub.2007.03.064.
33. **Figueiredo VC**, **Caldow MK**, **Massie V**, **Markworth JF**, **Cameron-Smith D**, **Blazevich AJ.** Ribosome biogenesis adaptation in resistance training-induced human skeletal muscle hypertrophy. *Am J Physiol Endocrinol Metab* 309: E72–E83, 2015. doi:10.1152/ajpendo.00050.2015.
34. **Nakada S**, **Ogasawara R**, **Kawada S**, **Maekawa T**, **Ishii N.** Correlation between ribosome biogenesis and the magnitude of hypertrophy in overloaded skeletal muscle. *PLoS One* 11: e0147284, 2016. doi:10.1371/journal.pone.0147284.
35. **Roberts MD**, **Mobley CB**, **Vann CG**, **Haun CT**, **Schoenfeld BJ**, **Young KC**, **Kavazis AN.** Synergist ablation-induced hypertrophy occurs more rapidly in the plantaris than soleus muscle in rats due to different molecular mechanisms. *Am J Physiol Regul Integr Comp Physiol* 318: R360–R368, 2020. doi:10.1152/ajpregu.00304.2019.
36. **Razi A**, **Ortega J.** Ribosomal proteins: their role in the assembly, structure and function of the ribosome. In: *Encyclopedia of Life Sciences*. Wiley, 2017, p. 1–12.
37. **Ubaida-Mohien C**, **Gonzalez-Freire M**, **Lyashkov A**, **Moaddel R**, **Chia CW**, **Simonsick EM**, **Sen R**, **Ferrucci L.** Physical activity associated proteomics of skeletal muscle: being physically active in daily life may protect skeletal muscle from aging. *Front Physiol* 10: 312, 2019. doi:10.3389/fphys.2019.00312.
38. **West DW**, **Marcotte GR**, **Chason CM**, **Juo N**, **Baehr LM**, **Bodine SC**, **Baar K.** Normal ribosomal biogenesis but shortened protein synthetic response to acute eccentric resistance exercise in old skeletal muscle. *Front Physiol* 9: 1915, 2018. doi:10.3389/fphys.2018.01915.
39. **Parry HA**, **Roberts MD**, **Kavazis AN.** Human skeletal muscle mitochondrial adaptations following resistance exercise training. *Int J Sports Med* 41: 349–359, 2020. doi:10.1055/a-1121-7851.
40. **MacDougall JD**, **Sale DG**, **Moroz JR**, **Elder GC**, **Sutton JR**, **Howald H.** Mitochondrial volume density in human skeletal muscle following heavy resistance training. *Med Sci Sports* 11: 164–166, 1979.
41. **Lüthi JM**, **Howald H**, **Claassen H**, **Rösler K**, **Vock P**, **Hoppeler H.** Structural changes in skeletal muscle tissue with heavy-resistance exercise. *Int J Sports Med* 7: 123–127, 1986. doi:10.1055/s-2008-1025748.
42. **Groennebaek T**, **Vissing K.** Impact of resistance training on skeletal muscle mitochondrial biogenesis, content, and function. *Front Physiol* 8: 713, 2017. doi:10.3389/fphys.2017.00713.
43. **Goldberg AL.** Protein synthesis during work-induced growth of skeletal muscle. *J Cell Biol* 36: 653–658, 1968. doi:10.1083/jcb.36.3.653.
44. **Robinson MM**, **Dasari S**, **Konopka AR**, **Johnson ML**, **Manjunatha S**, **Esponda RR**, **Carter RE**, **Lanza IR**, **Nair KS.** Enhanced protein translation underlies improved metabolic and physical adaptations to different exercise training modes in young and old humans. *Cell Metab* 25: 581–592, 2017. doi:10.1016/j.cmet.2017.02.009.
45. **Dolezal P**, **Likic V**, **Tachezy J**, **Lithgow T.** Evolution of the molecular machines for protein import into mitochondria. *Science* 313: 314–318, 2006. doi:10.1126/science.1127895.
46. **Makhnovskii PA**, **Zgoda VG**, **Bokov RO**, **Shagimardanova EI**, **Gazizova GR**, **Gusev OA**, **Lysenko EA**, **Kolpakov FA**, **Vinogradova**

OL, **Popov DV.** Regulation of proteins in human skeletal muscle: the role of transcription. *Sci Rep* 10: 3514, 2020. doi:10.1038/s41598-020-60578-2.

47. **Thomas AC**, **Stead CA**, **Burniston JG**, **Phillips SM.** Exercise-specific adaptations in human skeletal muscle: molecular mechanisms of making muscles fit and mighty. *Free Radic Biol Med* 223: 341–356, 2024. doi:10.1016/j.freeradbiomed.2024.08.010.
48. **Viggars MR**, **Wen Y**, **Peterson CA**, **Jarvis JC.** Automated cross-sectional analysis of trained, severely atrophied, and recovering rat skeletal muscles using MyoVision 2.0. *J Appl Physiol (1985)* 132: 593–610, 2022. doi:10.1152/japplphysiol.00491.2021.
49. **Viggars MR**, **Sutherland H**, **Cardozo CP**, **Jarvis JC.** Conserved and species-specific transcriptional responses to daily programmed resistance exercise in rat and mouse. *FASEB J* 37: e23299, 2023. doi:10.1096/fj.202301611R.
50. **Garrido C**, **Paul C**, **Seigneuric R**, **Kampinga HH.** The small heat shock proteins family: the long forgotten chaperones. *Int J Biochem Cell Biol* 44: 1588–1592, 2012. doi:10.1016/j.biocel.2012.02.022.
51. **Melkani GC**, **Cammarato A**, **Bernstein SI.** alphaB-crystallin maintains skeletal muscle myosin enzymatic activity and prevents its aggregation under heat-shock stress. *J Mol Biol* 358: 635–645, 2006. doi:10.1016/j.jmb.2006.02.043.
52. **Paulsen G**, **Lauritzen F**, **Bayer ML**, **Kalhovde JM**, **Ugelstad I**, **Owe SG**, **Hallen J**, **Bergersen LH**, **Raastad T.** Subcellular movement and expression of HSP27, αB-crystallin, and HSP70 after two bouts of eccentric exercise in humans. *J Appl Physiol (1985)* 107: 570–582, 2009 [Erratum in *J Appl Physiol* 108: 762, 2010]. doi:10.1152/japplphysiol.00209.2009.
53. **Jacko D**, **Bersiner K**, **Schulz O**, **Przyklenk A**, **Spahiu F**, **Höhfeld J**, **Bloch W**, **Gehlert S.** Coordinated alpha-crystallin B phosphorylation and desmin expression indicate adaptation and deadaptation to resistance exercise-induced loading in human skeletal muscle. *Am J Physiol Cell Physiol* 319: C300–C312, 2020. doi:10.1152/ajpcell.00087.2020.
54. **Zhu WG**, **Thomas AC**, **Wilson GM**, **McGlory C**, **Hibbert JE**, **Flynn CG**, **Sayed RK**, **Paez HG**, **Meinhold M**, **Jorgenson KW**, **You JS**, **Steinert ND**, **Lin KH**, **MacInnis MJ**, **Coon JJ**, **Phillips SM**, **Hornberger TA.** Identification of a resistance-exercise-specific signalling pathway that drives skeletal muscle growth. *Nat Metab* 7: 1404–1423, 2025. doi:10.1038/s42255-025-01298-7.
55. **Vaittinen S**, **Lukka R**, **Sahlgren C**, **Hurme T**, **Rantanen J**, **Lendahl U**, **Eriksson JE**, **Kalimo H.** The expression of intermediate filament protein nestin as related to vimentin and desmin in regenerating skeletal muscle. *J Neuropathol Exp Neurol* 60: 588–597, 2001. doi:10.1093/jnen/60.6.588.
56. **Schiaffino S**, **Rossi AC**, **Smerdu V**, **Leinwand LA**, **Reggiani C.** Developmental myosins: expression patterns and functional significance. *Skelet Muscle* 5: 22, 2015. doi:10.1186/s13395-015-0046-6.
57. **Kusić D**, **Connolly J**, **Kainulainen H**, **Semenova EA**, **Borisov OV**, **Larin AK**, **Popov DV**, **Generozov EV**, **Ahmetov II**, **Britton SL**, **Koch LG**, **Burniston JG.** Striated muscle-specific serine/threonine-protein kinase beta segregates with high versus low responsiveness to endurance exercise training. *Physiol Genomics* 52: 35–46, 2020. doi:10.1152/physiolgenomics.00103.2019.
58. **Murgia M**, **Toniolo L**, **Nagaraj N**, **Ciciliot S**, **Vindigni V**, **Schiaffino S**, **Reggiani C**, **Mann M.** Single muscle fiber proteomics reveals fiber-type-specific features of human muscle aging. *Cell Rep* 19: 2396–2409, 2017. doi:10.1016/j.celrep.2017.05.054.
59. **Fukuda S**, **Kaneshige A**, **Kaji T**, **Noguchi YT**, **Takemoto Y**, **Zhang L**, **Tsujikawa K**, **Kokubo H**, **Uezumi A**, **Maehara K**, **Harada A**, **Ohkawa Y**, **Fukada SI.** Sustained expression of HeyL is critical for the proliferation of muscle stem cells in overloaded muscle. *eLife* 8: e48284, 2019. doi:10.7554/eLife.48284.
60. **Mohanasundaram P**, **Coelho-Rato LS**, **Modi MK**, **Urbanska M**, **Lautenschläger F**, **Cheng F**, **Eriksson JE.** Cytoskeletal vimentin regulates cell size and autophagy through mTORC1 signaling. *PLoS Biol* 20: e3001737, 2022. doi:10.1371/journal.pbio.3001737.
61. **Chen YW**, **Nader GA**, **Baar KR**, **Fedele MJ**, **Hoffman EP**, **Esser KA.** Response of rat muscle to acute resistance exercise defined by transcriptional and translational profiling. *J Physiol* 545: 27–41, 2002. doi:10.1113/jphysiol.2002.021220.
62. **Levy S**, **Avni D**, **Hariharan N**, **Perry RP**, **Meyuhas O.** Oligopyrimidine tract at the 5' end of mammalian ribosomal protein mRNAs is required for their translational control. *Proc Natl Acad Sci USA* 88: 3319–3323, 1991. doi:10.1073/pnas.88.8.3319.
63. **Thoreen CC**, **Chantranupong L**, **Keys HR**, **Wang T**, **Gray NS**, **Sabatini DM.** A unifying model for mTORC1-mediated regulation of mRNA translation. *Nature* 485: 109–113, 2012. doi:10.1038/nature11083.
64. **Murach KA**, **Liu Z**, **Jude B**, **Figueiredo VC**, **Wen Y**, **Khadgi S**, **Lim S**, **Morena da Silva F**, **Greene NP**, **Lanner JT**, **McCarthy JJ**, **Vechetti IJ**, **von Walden F.** Multi-transcriptome analysis following an acute skeletal muscle growth stimulus yields tools for discerning global and MYC regulatory networks. *J Biol Chem* 298: 102515, 2022. doi:10.1016/j.jbc.2022.102515.
65. **van Riggelen J**, **Yetil A**, **Felsher DW.** MYC as a regulator of ribosome biogenesis and protein synthesis. *Nat Rev Cancer* 10: 301–309, 2010. doi:10.1038/nrc2819.
66. **Geiger T**, **Velic A**, **Macek B**, **Lundberg E**, **Kampf C**, **Nagaraj N**, **Uhlen M**, **Cox J**, **Mann M.** Initial quantitative proteomic map of 28 mouse tissues using the SILAC mouse. *Mol Cell Proteomics* 12: 1709–1722, 2013. doi:10.1074/mcp.M112.024919.
67. **Scalzo RL**, **Peltonen GL**, **Binns SE**, **Shankaran M**, **Giordano GR**, **Hartley DA**, **Klochak AL**, **Lonac MC**, **Paris HL**, **Szallar SE**, **Wood LM**, **Peelor FF 3rd**, **Holmes WE**, **Hellerstein MK**, **Bell C**, **Hamilton KL**, **Miller BF.** Greater muscle protein synthesis and mitochondrial biogenesis in males compared with females during sprint interval training. *FASEB J* 28: 2705–2714, 2014. doi:10.1096/fj.13-246595.
68. **Smith GI**, **Villareal DT**, **Sinacore DR**, **Shah K**, **Mittendorfer B.** Muscle protein synthesis response to exercise training in obese, older men and women. *Med Sci Sports Exerc* 44: 1259–1266, 2012. doi:10.1249/MSS.0b013e3182496a41.
69. **Miller BF**, **Hamilton KL**, **Majeed ZR**, **Abshire SM**, **Confides AL**, **Hayek AM**, **Hunt ER**, **Shipman P**, **Peelor FF 3rd**, **Butterfield TA**, **Dupont-Versteegden EE.** Enhanced skeletal muscle regrowth and remodelling in massaged and contralateral non-massaged hindlimb. *J Physiol* 596: 83–103, 2018. doi:10.1113/JP275089.
70. **Sklivas AB**, **Hettinger ZR**, **Rose S**, **Mantuano A**, **Confides AL**, **Rigsby S**, **Peelor FF 3rd**, **Miller BF**, **Butterfield TA**, **Dupont-Versteegden EE.** Responses of skeletal muscle to mechanical stimuli in female rats following and during muscle disuse atrophy. *J Appl Physiol (1985)* 138: 652–665, 2025. doi:10.1152/japplphysiol.00802.2024.